Physical Nature of Interactions in Zn^{II} Complexes with 2,2′-Bipyridyl: Quantum Theory of Atoms in Molecules (QTAIM), Interacting Quantum Atoms (IQA), Noncovalent Interactions (NCI), and Extended Transition State Coupled with Natural Orbitals for Chemical Valence (ETS-NOCV) Comparative Studies

Ignacy Cukrowski[a], Jurgens H. de Lange[a] and Mariusz Mitoraj[b]**

Supplementary Information

[a] Department of Chemistry, Faculty of Natural and Agricultural Sciences, University of Pretoria, Lynnwood Road, Pretoria 0002, South Africa

[b] K. Gumiński Department of Theoretical Chemistry, Faculty of Chemistry, Jagiellonian University, R. Ingardena 3, 30-060 Cracow, Poland

E-mails: ignacy.cukrowski@up.ac.za
jurgensdl@tuks.co.za
mitoraj@chemia.uj.edu.pl

Brief theoretical background

Due to the comparative nature of this study and to facilitate interpretation of interatomic interaction investigated in this work, it is of importance (and also convenience to a reader) to briefly outline basic theoretical principles of each method employed here.

QTAIM. Bader's Quantum Theory of Atoms in Molecules[1] (QTAIM) is among most cited real space methods (generally known as topological methods) which study the spatial distribution of scalar fields derived from reduced electron density matrices. Based on the atomic virial theorem, QTAIM provides a well-defined partitioning of an equilibrium molecule and its energy into real-space atomic (one-body) contributions; one partitioning scheme applies to all molecules. These atoms are quantum mechanical in origin, highly transferable and analogous to a molecular system with boundaries at infinity. According to QTAIM, there is always a characteristic point in 3D space of electron density topology of a molecule, called a bond critical point (BCP), which is found only between two atoms which are connected by an atomic interaction line (AIL). AIL is a line of local maximum density (termed in QTAIM as a bond path) and BCP is (i) a local minimum on the AIL where the AIL crosses the zero-flux inter-atomic surface (IAS), a boundary between two atoms defined by an atomic basin (a 3D attraction basin of the gradient field of the electron density, which is bounded by a zero flux surface of this field) and (ii) a local maximum on the IAS. It has been shown that the physics underlying bonded interactions in combination with the properties of the electron and energy densities at a bond critical point is useful in the study of the entire spectrum of bonding.[2,3] Hence, we analyse here the topology of the electron density of molecules being at equilibrium with a particular focus on atoms involved in intramolecular interactions. One must note that the requirement of the virial theorem to be <u>exactly</u> satisfied does not apply here as we do not analyse atomic energies. For the current work, we will call an AIL a bond path (defined by Bader as a necessary and sufficient condition for atoms to be bonded to one another[1]) only in the case when it

applies to generally accepted (one might say, based on an orthodox interpretation) bonding interactions, such as covalent or coordination bond. We do this to avoid unnecessary (when the aim of this work is concerned) controversy in the interpretation of a physical meaning of a bond path and a bond critical point.

IQA. The Interacting Quantum Atoms (IQA) approach of Blanco *et al*[4–6] is an energy decomposition scheme which (i) allows physical terms present in the Hamiltonian to be partitioned into atomic and interatomic contributions, (ii) considers all one- and two-electron energetic contributions, (iii) is fully consistent with the quantum theory of atoms in molecules; it is making use of an exhaustive partition of the 3D physical space into a set of QTAIM-defined atomic basins, Ω_A, and (iv) is free from the equilibrium geometry constraint of QTAIM (virial theorem does not apply in IQA). The IQA-defined energy decomposition scheme allows recovering the quantities of the most widely used energy decomposition schemes provided that one has many electron wave function with the desired accuracy, Ψ_e, needed to construct the (i) first-order (non-diagonal) density matrix and (ii) second-order (diagonal) matrix where the latter one is necessary to compute the most expensive potential energy term, V_{ee}. The main equation in partitioning of energy in the IQA method

$$\ldots E = \sum_{A} E_{self}^{A} + \frac{1}{2}\sum_{A}\sum_{B\neq A} E_{int}^{AB} \qquad (1)$$

states that the total energy of a molecule can be partitioned in two major contributions, namely (i) one-body self-energy term of an atom A, E_{self}^{A}, which carries all of the intra-atomic contributions (kinetic, T^A, nuclear attraction, V_{en}^{AA}, and two-electron repulsion, V_{ee}^{AA}),

$$E_{self}^{A} = T^{A} + V_{en}^{AA} + V_{ee}^{AA} \qquad (2)$$

and (ii) two-body pairwise additive interaction energy contribution between atom A and B, E_{int}^{AB}, which includes all inter-particle potentials (nucleus-nucleus, V_{nn}^{AB}, nucleus-electron, V_{ne}^{AB}, electron-

nucleus, $V_{\mathrm{en}}^{\mathrm{AB}}$, and electron-electron, $V_{\mathrm{ee}}^{\mathrm{AB}}$) coming from interatomic interaction energies of particles ascribed to atom A with particles ascribed to atom B

$$E_{\mathrm{int}}^{\mathrm{AB}} = V_{\mathrm{nn}}^{\mathrm{AB}} + V_{\mathrm{en}}^{\mathrm{AB}} + V_{\mathrm{ne}}^{\mathrm{AB}} + V_{\mathrm{ee}}^{\mathrm{AB}} \quad (3)$$

The interaction energy described by Eq. 3 can be seen as based on the physical interaction between the two systems (or atoms), which also takes into account the quantum nature of the electrons through the use of the second-order density matrix in the electron-electron repulsion. What is also important to stress is the fact that $E_{\mathrm{int}}^{\mathrm{AB}}$ equally applies to (i) atoms connected by a 'chemical bond', (ii) non-bonded atoms (e.g. when there is no QTAIM-defined bond path between them), or even (iii) intermolecular interactions, as it treats all of them on the same footing.

The second-order density matrix admits a natural partitioning into a Coulomb, Fock-Dirac exchange and correlation terms resulting in further partitioning of $V_{\mathrm{ee}}^{\mathrm{AB}}$,

$$V_{\mathrm{ee}}^{\mathrm{AB}} = V_{\mathrm{C}}^{\mathrm{AB}} + V_{\mathrm{X}}^{\mathrm{A|B}} + V_{\mathrm{corr}}^{\mathrm{A|B}} \quad (4)$$

and after substitution of Eq 4 into Eq 3 one obtains the total interaction energy between two atoms decomposed into six terms,

$$E_{\mathrm{int}}^{\mathrm{AB}} = V_{\mathrm{nn}}^{\mathrm{AB}} + V_{\mathrm{en}}^{\mathrm{AB}} + V_{\mathrm{ne}}^{\mathrm{AB}} + V_{\mathrm{C}}^{\mathrm{AB}} + V_{\mathrm{X}}^{\mathrm{AB}} + V_{\mathrm{corr}}^{\mathrm{AB}} \quad (5)$$

One should note that the first four terms (i) usually might be orders of magnitude larger than the last two terms and (ii) can be seen as of classical origin; hence it is useful and informative to combine them as

$$V_{\mathrm{cl}}^{\mathrm{AB}} = V_{\mathrm{nn}}^{\mathrm{AB}} + V_{\mathrm{en}}^{\mathrm{AB}} + V_{\mathrm{ne}}^{\mathrm{AB}} + V_{\mathrm{C}}^{\mathrm{AB}} \quad (6)$$

The $V_{\mathrm{cl}}^{\mathrm{AB}}$ classical energy term is the one where the cancellations between nucleus-nucleus, nucleus-electron, electron-nucleus, and Coulombic term of electron-electron interactions occur. For instance, when two neutral atoms are well separated then the classical term should be negligible, and

on atoms being closer it is expected to be positive and larger.[4,5] However, if the interactions between charged atoms (or molecules with significantly uneven intramolecular charge distribution) are considered, then the charge-charge classical interaction will be the decisive (most significant) contribution to $V_{\mathrm{cl}}^{\mathrm{AB}}$ which might become of an overall destabilizing (positive) or stabilizing (negative in value) nature to the interaction.[6]

Also, because (i) usually $V_{\mathrm{X}}^{\mathrm{AB}} >> V_{\mathrm{corr}}^{\mathrm{AB}}$ and (ii) separation of the exchange and correlation terms is arbitrary and can produce misleading results,[4] it is convenient to combine the last two terms in Eq 5 as the exchange-correlation contribution containing all of the quantum terms in the interaction between two atoms

$$V_{\mathrm{XC}}^{\mathrm{AB}} = V_{\mathrm{X}}^{\mathrm{AB}} + V_{\mathrm{corr}}^{\mathrm{AB}} \tag{7}$$

Finally, one can express the interatomic (or inter-molecular) interaction as a competition between two distinctively different, electrostatic and quantum, components,

$$E_{\mathrm{int}}^{\mathrm{AB}} = V_{\mathrm{cl}}^{\mathrm{AB}} + V_{\mathrm{XC}}^{\mathrm{AB}} \tag{8}$$

where these two components are (i) of comparable absolute values and (ii) can be used to classify the interaction as 'classically' of predominant ionic ($\left|V_{\mathrm{cl}}^{\mathrm{AB}}\right| >> \left|V_{\mathrm{XC}}^{\mathrm{AB}}\right|$), or covalent ($\left|V_{\mathrm{cl}}^{\mathrm{AB}}\right| << \left|V_{\mathrm{XC}}^{\mathrm{AB}}\right|$) nature. One must note that the energy contribution coming from $V_{\mathrm{XC}}^{\mathrm{AB}}$ is always stabilizing (often it can be seen as an electron sharing or spin pairing[4]). This means that the overall stabilizing or destabilizing nature of the interatomic interaction might greatly depend on the overall classical contribution coming from all electrostatic interactions, $V_{\mathrm{cl}}^{\mathrm{AB}}$.

Non-covalent interaction (NCI) method.[7–10] It provides an index of inter- and intramolecular stabilizing (e.g. hydrogen bonds) and destabilizing (steric repulsion) interactions; all non-covalent interactions (this also includes the so-called 'nonbonded' interactions) emerge in the NCI method as continuous 3-D surfaces rather than close contacts between atom pairs. NCI can use either the self-

consistent and fully quantum-mechanical or promolecular electron density, ρ, for simultaneous analysis and visualization of a wide range of noncovalent interactions in real space as opposed to assigning them in terms of pairwise distances between atoms based on their van der Waals radii.[11]

The NCI method is making use of the reduced density gradient (RDG) which, in density functional theory (DFT), describes the deviation from a homogeneous electron distribution[12–14]

$$s(\rho) = \frac{1}{C_F} \frac{|\nabla \rho|}{\rho^{4/3}} \tag{9}$$

where $C_F = 2(3\pi^2)^{1/3}$ is a constant and the 4/3 exponent of the density ensures that $s(\rho)$ is a dimensionless quantity. The RDG has interesting properties, namely (i) in density tails (far from the molecule where the density is exponentially approaching zero more rapidly than the gradient in numerator) $s(\rho)$ will have very large positive values, (ii) it will assume values approaching zero when an inter-atomic interaction is present, (iii) when there is an overlap between atomic orbitals, troughs appear in the 2D $s(\rho)$ vs. ρ diagram in the low-density, low-gradient region, (iv) the low $s(\rho)$ regions, when traced back to molecular space, give rise to isosurfaces which can be used to visualize the weak interactions in the system, and (v) the density values of the low-gradient trough can be used as an indicator of the interaction strength.

However, both attractive and repulsive interactions (i.e., hydrogen-bonding and steric repulsion) appear in the same region of density/reduced gradient space and to distinguish between them an analysis of the Laplacian is performed. To this end, on the basis of the divergence theorem,[15] the sign of the Laplacian ($\nabla^2\rho$) of the density is used as it indicates whether the net gradient flux of density is concentrated ($\nabla^2\rho < 0$) or depleted ($\nabla^2\rho > 0$) relative to the surroundings in an infinitesimal volume around a point in the 3D space. For non-covalent, hence weaker interactions, the Laplacian in the interatomic region is dominated by the positive contribution,[2] independently of whether they are bonding or nonbonding. Hence, to distinguish between them, contributions to $\nabla\rho^2$

along the axes of its maximal variation must be analysed.[2] This is achieved by decomposing the Laplacian into a sum of three eigenvalues λ_i of the electron-density Hessian (second derivative) matrix contributions ($\nabla\rho^2 = \lambda_1 + \lambda_2 + \lambda_3$, where $\lambda_1 \leq \lambda_2 \leq \lambda_3$ along the three principal axes of maximal variation; λ_3 varies along the inter-nuclear direction, while λ_1 and λ_2 report the variation of density in the plane normal to the λ_3 eigenvector).

This means that the sign of the second Hessian eigenvalue (λ_2) can be used to distinguish bonded ($\lambda_2 < 0$, indicative of charge accumulation) from nonbonded ($\lambda_2 > 0$, e.g. in case of charge depletion between crowded, or in close proximity, atoms which do not form a bond; in classical chemistry it is interpreted as steric repulsion) interactions, whereas the density itself provides information about their strength. Since non-covalent interactions are characterized by low density and reduced gradient values, they can be located by generating gradient isosurfaces enclosing the corresponding regions of real space and their type can be recovered by the values of sign(λ_2)×ρ in these regions; (i) negative values of sign(λ_2)×ρ are indicative of attractive interactions (e.g. hydrogen bonding), (ii); positive value of sign(λ_2)×ρ points at nonbonding interaction (steric repulsion), and (iii) values near zero indicate very weak, van der Waals interactions.

Clearly, non-covalent interactions (i) have unique signatures and their presence can be revealed solely from the electron density when 2D plots of the reduced density gradient vs. sign(λ_2)×ρ are generated and (ii) are highly nonlocal and appear in real space as low-gradient isosurfaces with low densities.

The ETS-NOCV method. The Natural Orbitals for Chemical Valence (NOCV) have been derived[16] from the Nalewajski-Mrozek valence theory and it has been shown[16,17] that the natural orbitals for chemical valence pairs (ψ_{-k},ψ_k) decompose the deformation density $\Delta\rho$ into NOCV-contributions, $\Delta\rho_k$,:

$$\Delta\rho(r) = \sum_{k=1}^{M/2} v_k[-\psi_{-k}^2(r) + \psi_k^2(r)] = \sum_{k=1}^{M/2} \Delta\rho_k(r) \quad (10)$$

where v_k and M stand for the NOCV eigenvalues and the number of basis functions, respectively. Visual inspection of deformation density plots ($\Delta\rho_k$) helps to attribute symmetry and the direction of the charge flow. In addition, information gained from the analysis of the deformation density plots can be enriched by providing the energetic estimations, $\Delta E_{orb}(k)$, for each $\Delta\rho_k$ within ETS-NOCV scheme.[17] The basic concept of ETS scheme involves partitioning of the total bonding energy ΔE_{total} between interacting fragments (or atoms) into four components:

$$\Delta E_{total} = \Delta E_{dist} + \Delta E_{elstat} + \Delta E_{Pauli} + \Delta E_{orb} = \Delta E_{dist} + \Delta E_{int} \quad (11)$$

The first component, ΔE_{dist}, referred to as the distortion term, represents the amount of energy required to promote the separated fragments from their equilibrium geometry to the structure they will take up in the combined molecule; it can also be seen as strain energy. The second term, ΔE_{elstat}, corresponds to the classical electrostatic interaction between the promoted fragments as they are brought to their positions in the final complex. The third term, ΔE_{Pauli}, accounts for the repulsive Pauli interaction between occupied orbitals on the two fragments in the combined molecule. The second and third term (ΔE_{elstat} and ΔE_{Pauli}) are often combined into the steric interaction (ΔE_{steric}).[17–20] Finally, the last and stabilizing term, ΔE_{orb}, represents the interactions between the occupied molecular orbitals of one fragment with the unoccupied molecular orbitals of the other fragment as well as mixing of occupied and virtual orbitals within the same fragment (inner-fragment polarization). This energy term, ΔE_{orb}, may be linked to the electronic bonding effect coming from the formation of a chemical bond. The three last terms (ΔE_{elstat}, ΔE_{Pauli}, ΔE_{orb}) very often are combined into the instantaneous interaction energy, ΔE_{int}, as it describes the interaction between the fragments in the geometry of the complex.

In the combined ETS-NOCV scheme[16] the orbital interaction ΔE_{orb} is expressed in terms of NOCV's eigenvalues, v_k, as:

$$\Delta E_{orb} = \sum_k \Delta E_{orb}(k) = \sum_{k=1}^{M/2} v_k [-F_{-k,-k}^{TS} + F_{k,k}^{TS}] \quad (12)$$

where $F_{i,i}^{TS}$ are diagonal Kohn-Sham matrix elements defined over NOCV with respect to the transition state density (at the midpoint between density of the molecule and the sum of fragment densities). The above components $\Delta E_{orb}(k)$ provide the energetic estimation of $\Delta\rho_k$ that may be related to the importance of a particular electron flow channel for the bonding between the considered molecular fragments.

References

(1) Bader, R. F. W. *Atoms in Molecules: A Quantum Theory*; Oxford University Press: Oxford, 1990.

(2) Bader, R. F. W.; Essén, H. *J. Chem. Phys.* **1984**, *80*, 1943–1960.

(3) Cukrowski, I.; Govender, K. K.; Mitoraj, M. P.; Srebro, M. *J. Phys. Chem. A* **2011**, *115*, 12746–12757.

(4) Blanco, M. A.; Pendás, A. M.; Francisco, E. *J. Chem. Theory Comput.* **2005**, *1*, 1096–1109.

(5) Francisco, E.; Pendás, A. M.; Blanco, M. A. *J. Chem. Theory Comput.* **2006**, *2*, 90–102.

(6) Pendás, A. M.; Blanco, M. A.; Francisco, E. *J. Comput. Chem.* **2007**, *28*, 161–184.

(7) Johnson, E. R.; Keinan, S.; Mori-Sánchez, P.; Contreras-García, J.; Cohen, A. J.; Yang, W. *J. Am. Chem. Soc.* **2010**, *132*, 6498–6506.

(8) Contreras-García, J.; Johnson, E. R.; Keinan, S.; Chaudret, R.; Piquemal, J. P.; Beratan, D.; Yang, W. *J. Chem. Theory Comput*. **2011**, *7*, 625–632.

(9) Gillet, N.; Chaudret, R.; Contreras-García, J.; Yang, W.; Silvi, B.; Piquemal, J. P. *J. Chem. Theory Comput.* **2012**, *8*, 3993−3997.

(10) Contreras-García, J.; Yang, W.; Johnson, E. R. *J. Phys. Chem. A* **2011**, *115*, 12983–12990.

(11) Klein, R. A. *Chem. Phys. Lett.* **2006**, *425*, 128–133.

(12) Hohenberg, P.; Kohn, W. *Phys. Rev. B* **1964**, *136*, 864–871.

(13) Becke, A. D. *Modern Electronic Structure Theory.* Yarkony, D. R., Ed.; World Scientific: River Edge, NJ, **1995**; pp 1022–1046.

(14) Cohen, A. J.; Mori-Sánchez, P.; Yang, W. *Science* **2008**, *321*, 792–794.

(15) Arfken, G. *Mathematical Methods for Physicists*; Academic Press: Orlando, FL, 1985.

(16) Mitoraj, M.; Michalak, A. *J. Mol. Model*. **2007**, *13,* 347–355.

(17) Mitoraj, M.; Michalak, A.; Ziegler, T. *J. Chem. Theory Comput.* **2009**, *5*, 962–975.

(18) Ziegler, T.; Rauk, A. *Inorg. Chem.* **1979**, *18*, 1755–1759.

(19) Ziegler, T.; Rauk, A. *Inorg. Chem.* **1979**, *18*, 1558–1565.

(20) Ziegler, T.; Rauk, A. *Theor. Chim. Acta* **1977**, *46*, 1–10.

Table S1. Selected structural data for equilibrium geometries of the ZnL_n complexes

Complex	Bond length (Å)		Bite angle (deg)		Torsion (deg)		Close contacts (Å)	
ZnL	Zn–O1	2.162	N5-Zn-N6	79.13	N5-C15-C16-N6	-1.44	C**H14•••H18**C	2.048
	Zn–O2	2.194			**H14**-C13-C15-C16	0.05	CH8•••O1	2.544
	Zn–O3	2.162			**H18**-C17-C16-C15	0.05	CH24•••O3	2.544
	Zn–O4	2.194						
	average:	*2.178*						
	std dev:	*0.018*						
	Zn–N5	2.107						
	Zn–N6	2.107						
ZnL_2	Zn–N1	2.153	N1-Zn-N2	77.40	N1-C13-C14-N2	0.31	C**H16•••H18**C	2.031
	Zn–N2	2.143	N3-Zn-N4	77.48	**H16**-C15-C13-C14	-0.45	C**H32•••H36**C	2.036
	Zn–N3	2.149			**H18**-C17-C14-C13	0.52	CH24•••O6	2.451
	Zn–N4	2.143			N3-C33-C34-N4	1.89	CH42•••O5	2.455
	average:	*2.147*			**H32**-C31-C33-C34	0.18	CH26•••N2	2.810
	std dev:	*0.005*			**H36**-C35-C34-C33	0.79	CH8•••N4	2.819
	Zn–O5	2.273						
	Zn–O6	2.276						
ZnL_3	Zn–N55	2.217	N55-Zn-N56	74.76	N55-C9-C10-N56	0.76	C**H8•••H12**C	2.013
	Zn–N56	2.216	N57-Zn-N58	74.77	**H8**-C7-C9-C10	0.07	C**H26•••H30**C	2.007
	Zn–N57	2.215	N59-Zn-N60	74.78	**H12**-C11-C10-C9	-0.35	C**H44•••H48**C	2.011
	Zn–N58	2.220			N57-C27-C28-N58	0.38	CH20•••N55	2.668
	Zn–N59	2.218			**H26**-C25-C27-C28	0.10	CH54•••N56	2.671
	Zn–N60	2.217			**H30**-C29-C28-C27	0.00	CH38•••N57	2.684
	average:	*2.217*			N59-C45-C46-N60	1.61	CH18•••N58	2.685
	std dev:	*0.002*			**H44**-C43-C45-C46	0.15	CH2•••N59	2.685
					H48-C47-C46-C45	-0.34	CH36•••N60	2.672

Table S2. Cartesian coordinates for the $[ZnL(H_2O)_4]^{2+}$ complex (L = 2,2′-bipyridyl)

Standard orientation					
Center	Atomic	Atomic	Coordinates (Angstroms)		
Number	Number	Type	X	Y	Z
1	8	0	-2.7284	-1.5638	0.0093
2	8	0	-1.6885	-0.0051	2.1465
3	8	0	-2.7285	1.5636	-0.0093
4	8	0	-1.6885	0.0049	-2.1464
5	7	0	0.3884	-1.3413	0.039
6	7	0	0.3883	1.3414	-0.039
7	6	0	0.3029	-2.6759	0.0598
8	1	0	-0.6945	-3.0912	0.0732
9	6	0	1.4249	-3.4886	0.06
10	1	0	1.3138	-4.5629	0.0785
11	6	0	2.6754	-2.8858	0.0345
12	1	0	3.5753	-3.485	0.0317
13	6	0	2.7642	-1.5004	0.0089
14	1	0	3.7317	-1.0238	-0.0136
15	6	0	1.5961	-0.7435	0.0132
16	6	0	1.596	0.7436	-0.0133
17	6	0	2.7641	1.5005	-0.009
18	1	0	3.7316	1.0241	0.0135
19	6	0	2.6752	2.886	-0.0345
20	1	0	3.5751	3.4852	-0.0318
21	6	0	1.4247	3.4887	-0.0601
22	1	0	1.3135	4.563	-0.0785
23	6	0	0.3027	2.6759	-0.0598
24	1	0	-0.6947	3.0912	-0.0732
25	1	0	-3.417	-1.5173	-0.6684
26	1	0	-3.2011	-1.6273	0.8513
27	1	0	-1.1748	-0.6202	2.6883
28	1	0	-1.6211	0.8442	2.6055
29	1	0	-3.2013	1.627	-0.8512
30	1	0	-3.4171	1.5171	0.6685
31	1	0	-1.6211	-0.8443	-2.6055
32	1	0	-1.1749	0.6201	-2.6883
33	30	0	-1.2358	0	0

Molecular Electronic Energy: -2580.08621989 au

Table S3. Cartesian Coordinates for the $[ZnL_2(H_2O)_2]^{2+}$ Complex (L = 2,2′-Bipyridyl)

Standard orientation					
Center Number	Atomic Number	Atomic Type	Coordinates (Angstroms) X	Y	Z
1	7	0	-0.9093	-1.4706	0.5552
2	7	0	-2.0434	0.6451	-0.6517
3	7	0	0.9088	1.4651	0.5628
4	7	0	2.0436	-0.6407	-0.6593
5	8	0	-0.3424	-1.3276	-2.5354
6	8	0	0.3439	1.355	-2.5237
7	6	0	-0.285	-2.5157	1.1073
8	1	0	0.7599	-2.6377	0.8613
9	6	0	-0.9261	-3.4072	1.9527
10	1	0	-0.3817	-4.2396	2.3744
11	6	0	-2.269	-3.1959	2.2345
12	1	0	-2.8072	-3.8671	2.8893
13	6	0	-2.2143	-1.2608	0.8155
14	6	0	-2.8409	-0.0877	0.1502
15	6	0	-2.9211	-2.1132	1.6604
16	1	0	-3.9654	-1.9433	1.8701
17	6	0	-4.1818	0.2486	0.3246
18	1	0	-4.8198	-0.3378	0.9669
19	6	0	-4.6986	1.3527	-0.3379
20	1	0	-5.7369	1.6247	-0.2088
21	6	0	-3.8693	2.0965	-1.167
22	1	0	-4.2312	2.961	-1.7042
23	6	0	-2.5465	1.7041	-1.2967
24	1	0	-1.864	2.2428	-1.9378
25	6	0	0.2839	2.5082	1.1173
26	1	0	-0.7651	2.6212	0.8841
27	6	0	0.9272	3.4059	1.9545
28	1	0	0.3802	4.233	2.3832
29	6	0	2.276	3.2081	2.2169
30	1	0	2.8168	3.8855	2.8631
31	6	0	2.9293	2.1277	1.6393
32	1	0	3.9786	1.9701	1.833
33	6	0	2.2175	1.2633	0.8103
34	6	0	2.8401	0.0847	0.1507
35	6	0	4.175	-0.2659	0.3413
36	1	0	4.8095	0.3105	0.9961
37	6	0	4.6891	-1.3722	-0.3205
38	1	0	5.723	-1.6552	-0.1798
39	6	0	3.8625	-2.1046	-1.1623
40	1	0	4.2226	-2.9693	-1.7002
41	6	0	2.5438	-1.702	-1.3025
42	1	0	1.8624	-2.2349	-1.9494

Standard orientation					
Center	**Atomic**	**Atomic**	**Coordinates (Angstroms)**		
Number	**Number**	**Type**	**X**	**Y**	**Z**
43	1	0	0.8967	0.9448	-3.2033
44	1	0	0.7707	2.2023	-2.3389
45	1	0	-0.9049	-0.9088	-3.2012
46	1	0	-0.7694	-2.1755	-2.3531
47	30	0	0.0004	0.0032	-0.7246

Molecular Electronic Energy: -2922.51597175 au

Table S4. Cartesian Coordinates for the $[ZnL_3]^{2+}$ Complex (L = 2,2′-Bipyridyl)

Standard orientation					
Center Number	Atomic Number	Atomic Type	Coordinates (Angstroms)		
			X	Y	Z
1	6	0	-1.40207	-1.64497	-2.33947
2	1	0	-0.39724	-1.62114	-2.73541
3	6	0	-2.42222	-2.27121	-3.03819
4	1	0	-2.21734	-2.73989	-3.99007
5	6	0	-3.69338	-2.27697	-2.48014
6	1	0	-4.51849	-2.75479	-2.98993
7	6	0	-3.89454	-1.66278	-1.25246
8	1	0	-4.87781	-1.66428	-0.80905
9	6	0	-2.81906	-1.05154	-0.60734
10	6	0	-2.95952	-0.37681	0.710249
11	6	0	-4.17183	-0.32453	1.39812
12	1	0	-5.06176	-0.77453	0.986819
13	6	0	-4.23066	0.31464	2.627853
14	1	0	-5.16431	0.360527	3.171296
15	6	0	-3.07963	0.894651	3.144157
16	1	0	-3.07781	1.404577	4.096791
17	6	0	-1.91225	0.807	2.402173
18	1	0	-0.99498	1.248219	2.763739
19	6	0	-0.86565	2.030244	-2.28001
20	1	0	-1.36787	1.149496	-2.6528
21	6	0	-0.93963	3.231065	-2.96817
22	1	0	-1.5017	3.293103	-3.88887
23	6	0	-0.2784	4.331741	-2.44055
24	1	0	-0.31036	5.288729	-2.94304
25	6	0	0.430065	4.190194	-1.25656
26	1	0	0.946718	5.039648	-0.8381
27	6	0	0.460971	2.949593	-0.62021
28	6	0	1.194113	2.727119	0.653853
29	6	0	1.891358	3.746505	1.301616
30	1	0	1.920885	4.743891	0.89178
31	6	0	2.551241	3.472203	2.490483
32	1	0	3.092982	4.25468	3.003863
33	6	0	2.501186	2.185478	3.009732
34	1	0	2.993657	1.926745	3.936106
35	6	0	1.787485	1.22439	2.311351
36	1	0	1.72113	0.21159	2.680461
37	6	0	2.05581	-0.28349	-2.40092
38	1	0	1.51013	0.578379	-2.75671
39	6	0	3.102706	-0.81283	-3.13952
40	1	0	3.380656	-0.36527	-4.08315
41	6	0	3.771961	-1.9179	-2.63137

Standard orientation					
Center	**Atomic**	**Atomic**	**Coordinates (Angstroms)**		
Number	**Number**	**Type**	**X**	**Y**	**Z**
42	1	0	4.59577	-2.36187	-3.17296
43	6	0	3.370347	-2.45041	-1.41509
44	1	0	3.883763	-3.30914	-1.01212
45	6	0	2.306459	-1.86518	-0.72861
46	6	0	1.825637	-2.37935	0.581266
47	6	0	2.42708	-3.46	1.226953
48	1	0	3.270635	-3.96839	0.786649
49	6	0	1.932769	-3.88466	2.451444
50	1	0	2.394144	-4.7179	2.963319
51	6	0	0.843748	-3.226	3.005812
52	1	0	0.422911	-3.52346	3.955391
53	6	0	0.295274	-2.16298	2.305248
54	1	0	-0.55345	-1.62316	2.698674
55	7	0	-1.59023	-1.04891	-1.15745
56	7	0	-1.84802	0.186083	1.219808
57	7	0	-0.18437	1.887761	-1.13838
58	7	0	1.149949	1.482749	1.165096
59	7	0	1.664059	-0.79285	-1.22817
60	7	0	0.771816	-1.74474	1.127776
61	30	0	-0.0103	-0.00619	-0.00379

Molecular Electronic Energy: -3264.94124288

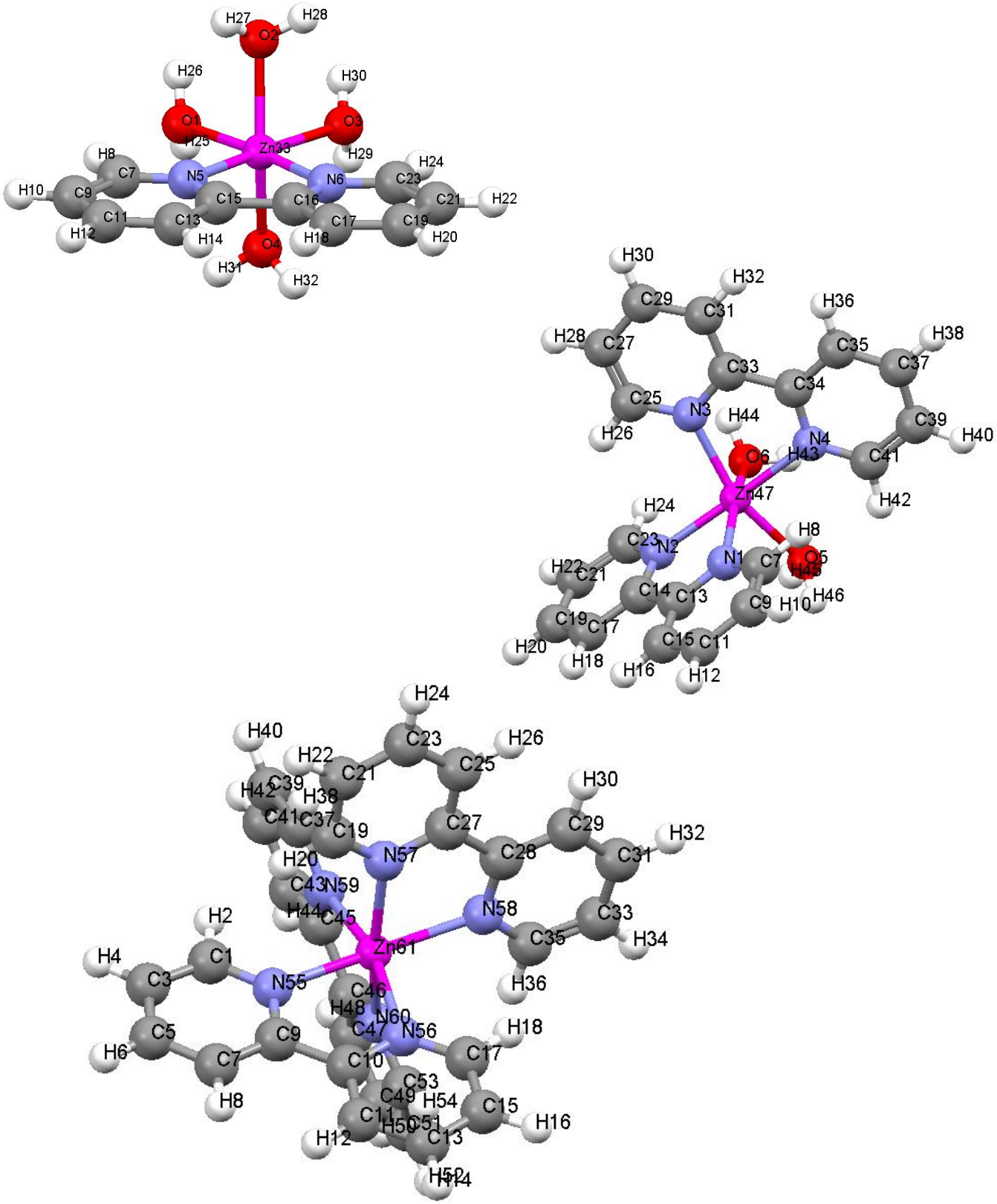

Figure S1. Ball and stick representations of ZnL, ZnL_2 and ZnL_3 complexes.

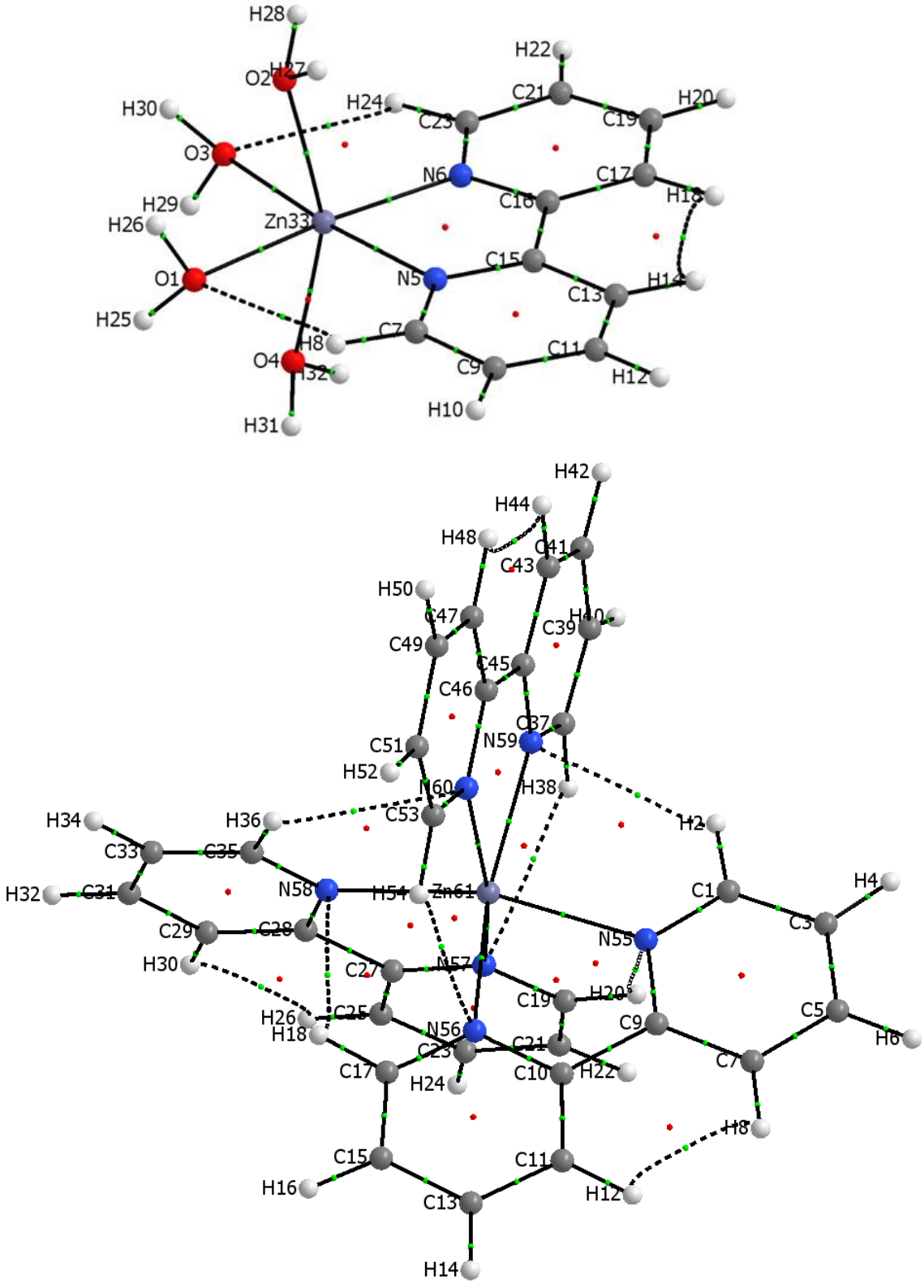

Figure S2. Molecular graphs of the ZnL and ZnL_3 complexes.

Table S5. Topological data at the BCP for all coordination bonds in Zn^{II} complexes with 2,2´-bipyridyl (L) optimized at X3LYP[a]

Complex	Atoms	$\rho(r)$	$\nabla^2\rho(r)$	$V(r)$	$G(r)$	$H(r)$	$\lvert V(r)\rvert/G(r)$
ZnL	Zn–N5	0.07049	0.25214	-0.09374	0.07839	-0.01535	1.19583
	Zn–N6	0.07050	0.25216	-0.09374	0.07839	-0.01535	1.19583
	Average	*0.07049*	*0.25215*	*-0.09374*	*0.07839*	*-0.01535*	*1.19583*
	Zn–O1	0.05179	0.21854	-0.06855	0.06159	-0.00696	1.11298
	Zn–O2	0.04798	0.19761	-0.06256	0.05598	-0.00658	1.11750
	Zn–O3	0.05179	0.21860	-0.06857	0.06161	-0.00696	1.11295
	Zn–O4	0.04799	0.19768	-0.06258	0.05600	-0.00658	1.11747
	Average	*0.04989*	*0.20811*	*-0.06556*	*0.05880*	*-0.00677*	*1.11523*
ZnL_2	Zn–N1	0.06353	0.21913	-0.08205	0.06841	-0.01363	1.19928
	Zn–N2	0.06512	0.22452	-0.08426	0.07019	-0.01406	1.20036
	Zn–N3	0.06408	0.22207	-0.08303	0.06928	-0.01376	1.19860
	Zn–N4	0.06513	0.22464	-0.08430	0.07023	-0.01407	1.20032
	Average	*0.06446*	*0.22259*	*-0.08341*	*0.06953*	*-0.01388*	*1.19964*
	Zn-O5	0.04081	0.15334	-0.05033	0.04433	-0.00600	1.13533
	Zn–O6	0.04048	0.15193	-0.04985	0.04392	-0.00593	1.13508
	Average	*0.04065*	*0.15264*	*-0.05009*	*0.04412*	*-0.00597*	*1.13520*
ZnL_3	Zn–N55	0.05560	0.18015	-0.06872	0.05688	-0.01184	1.20819
	Zn–N56	0.05568	0.18055	-0.06885	0.05699	-0.01186	1.20802
	Zn–N57	0.05586	0.18139	-0.06914	0.05724	-0.01190	1.20783
	Zn–N58	0.05521	0.17832	-0.06807	0.05633	-0.01175	1.20855
	Zn–N59	0.05542	0.17931	-0.06841	0.05662	-0.01179	1.20828
	Zn–N60	0.05558	0.18008	-0.06869	0.05685	-0.01183	1.20816
	Average	*0.05556*	*0.17996*	*-0.06865*	*0.05682*	*-0.01183*	*1.20817*

[a] $\rho(r)$, $\nabla^2\rho(r)$, $V(r)$, $G(r)$, and $H(r)$ - all in atomic units.

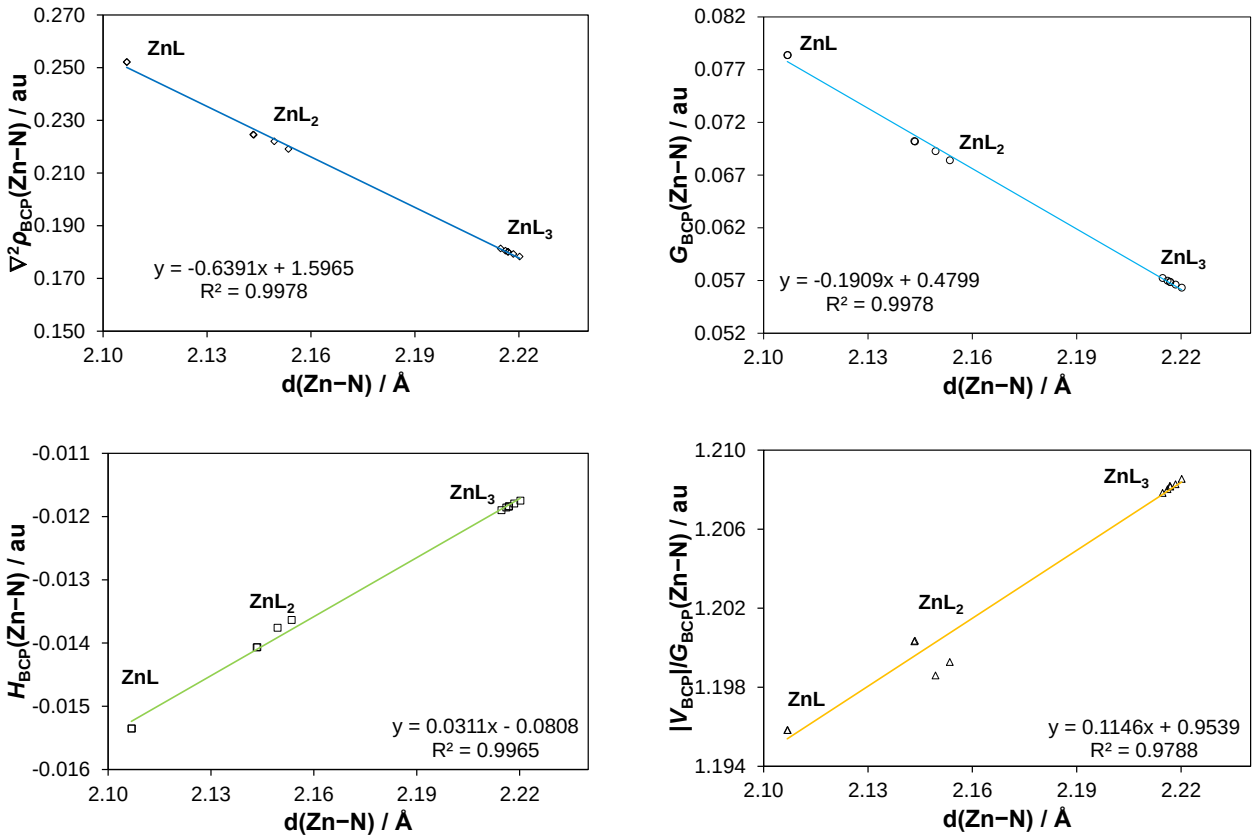

Figure S3. Additional relationships between bond lengths and topological properties at the BCP for Zn–N bonds.

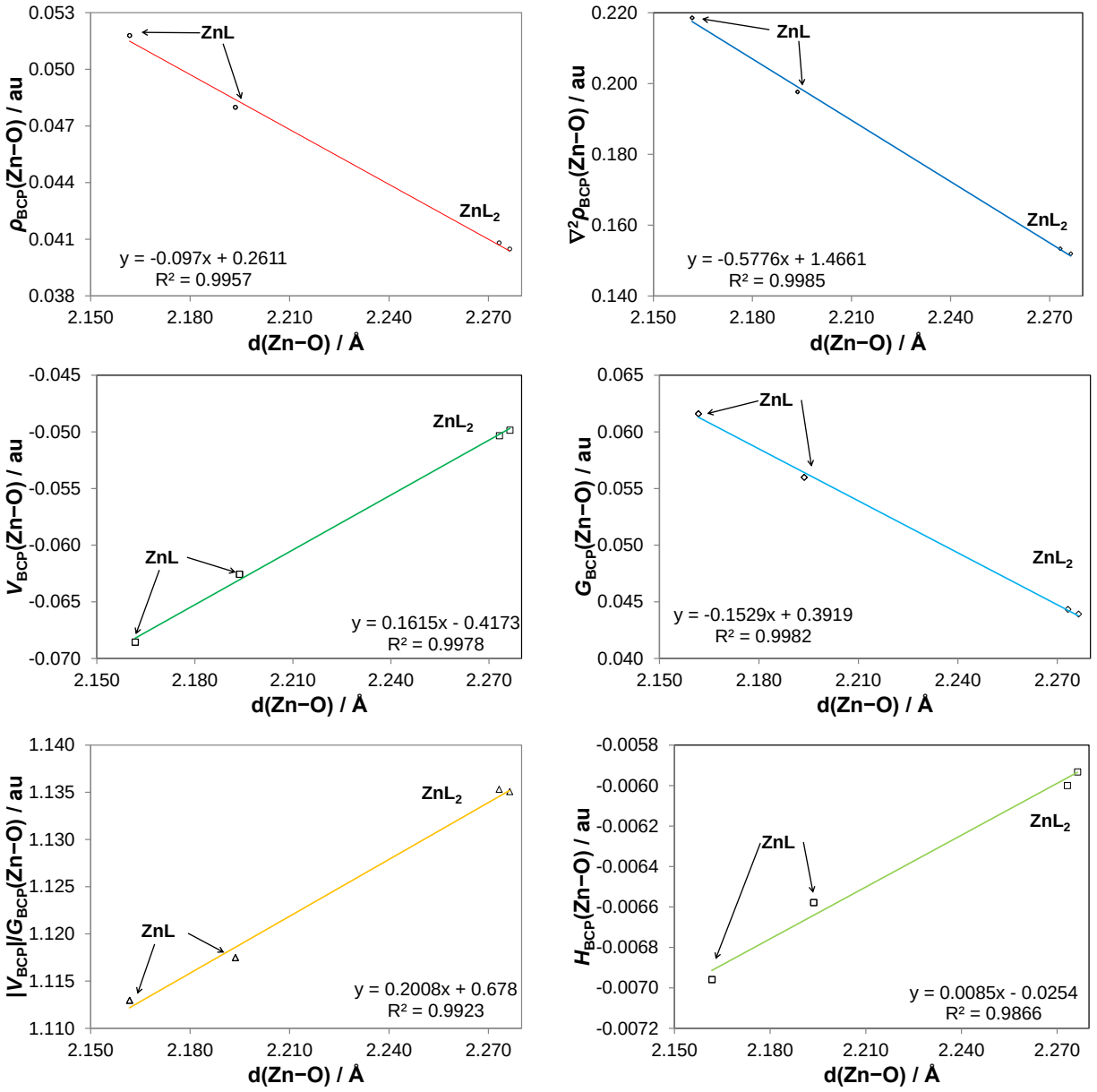

Figure S4 Relationships between bond lengths and topological properties at the BCP for Zn–O bonds.

Table S6. Topological data at the BCP for all intramolecular interactions in Zn^{II} complexes with 2,2´-bipyridyl (L) optimized at X3LYP[a]

Complex	Atoms	$\rho(r)$	$\nabla^2\rho(r)$	$V(r)$	$G(r)$	$H(r)$	$\lvert V(r)\rvert/G(r)$
ZnL	CH8–O1	0.00862	0.03082	-0.00546	0.00658	0.00112	0.82974
	CH24–O3	0.00862	0.03082	-0.00546	0.00658	0.00112	0.82973
	Average	*0.00862*	*0.03082*	*-0.00546*	*0.00658*	*0.00112*	*0.82973*
	CH14–H18C	0.01142	0.04390	-0.00652	0.00875	0.00222	0.745684
ZnL_2	CH42–O5	0.00981	0.03577	-0.00630	0.00762	0.00132	0.82630
	CH24–O6	0.00993	0.03606	-0.00636	0.00769	0.00133	0.82744
	Average	*0.00987*	*0.03592*	*-0.00633*	*0.00765*	*0.00133*	*0.82687*
	CH26–N2	0.00599	0.02016	-0.00341	0.00422	0.00081	0.80718
	CH8–N4	0.00590	0.01986	-0.00336	0.00416	0.00080	0.80669
	Average	*0.00595*	*0.02001*	*-0.00338*	*0.00419*	*0.00081*	*0.80693*
	CH16–H18C	0.01180	0.04517	-0.00674	0.00902	0.00227	0.74776
	CH36–H32C	0.01170	0.04483	-0.00668	0.00895	0.00226	0.74727
	Average	*0.01175*	*0.04500*	*-0.00671*	*0.00898*	*0.00227*	*0.74751*
ZnL_3	CH20–N55	0.00775	0.02510	-0.00429	0.00528	0.00100	0.81156
	CH54–N56	0.00770	0.02498	-0.00425	0.00525	0.00100	0.80950
	CH38–N57	0.00753	0.02444	-0.00417	0.00514	0.00097	0.81123
	CH18–N58	0.00750	0.02433	-0.00414	0.00511	0.00097	0.81048
	CH2–N59	0.00752	0.02436	-0.00415	0.00512	0.00097	0.81048
	CH36–N60	0.00773	0.02505	-0.00426	0.00526	0.00100	0.81000
	Average	*0.00763*	*0.02471*	*-0.00421*	*0.00519*	*0.00099*	*0.81024*
	CH12–H8C	0.01222	0.04661	-0.00699	0.00932	0.00233	0.75014
	CH30–H26C	0.01234	0.04704	-0.00707	0.00941	0.00235	0.75064
	CH48–H44C	0.01230	0.04688	-0.00704	0.00938	0.00234	0.75049
	Average	*0.01230*	*0.04688*	*-0.00704*	*0.00938*	*0.00234*	*0.75049*

[a] $\rho(r)$, $\nabla^2\rho(r)$, $V(r)$, $G(r)$, and $H(r)$ - all in atomic units.

Table S7. Decomposition of two-bodied interaction energies within the IQA framework for all relevant bonds in Zn^{II} complexes with 2,2´-bipyridyl

Complex	**Atoms**	**d(A–B)**	V_{ne}^{AB}	V_{en}^{AB}	V_{nn}^{AB}	V_{C}^{AB}	V_{cl}^{AB}	V_{XC}^{AB}	E_{Int}^{AB}	$V_{XC}^{AB} / E_{Int}^{AB}$
		Å	*au*	*au*	*au*	*au*	*kcal·mol*$^{-1}$	*kcal·mol*$^{-1}$	*kcal·mol*$^{-1}$	*kcal·mol*$^{-1}$
ZnL	*CH···HC*	*2.06*	-0.2472	-0.2472	0.2569	0.2375	-0.02	-2.48	-2.5	0.993
	CH···O	*2.6*	-1.7008	-1.7008	1.6285	1.7542	-11.86	-2.64	-14.5	0.182
	C-C	*1.497*	-11.4042	-11.4042	12.7218	10.2391	95.69	-193.43	-97.74	1.979
	Zn-N5	*2.145*	-56.0668	-56.0668	51.8045	59.7401	-369.65	-40.14	-409.79	0.098
	Zn-N6	*2.145*	-56.0670	-56.0670	51.8046	59.7402	-369.65	-40.14	-409.79	0.098
	Zn-O1	*2.157*	-61.8194	-61.8194	58.8847	64.2786	-298.43	-28.04	-326.47	0.086
	N5-N6	*2.673*	-11.8316	-11.8316	9.7005	14.4307	293.69	-7.03	286.67	–0.025
ZnL_2	*CH···HC*	*2.05*	-0.2488	-0.2488	0.2581	0.239	-0.23	-2.51	-2.74	0.916
	CH···O	*2.502*	-1.7656	-1.7656	1.6917	1.8195	-12.47	-3.26	-15.73	0.207
	CH···N	*2.879*	-1.3988	-1.3988	1.2866	1.4953	-9.91	-1.64	-11.56	0.142
	C-C	*1.497*	-11.4030	-11.4030	12.7264	10.233	96.27	-193.41	*-97.15*	1.991
	Zn-N1	2.183	-55.1408	-55.1408	50.9086	58.8099	-353.41	-36.73	-390.14	0.094
	Zn-N2	2.182	-55.1524	-55.1524	50.9243	58.8145	-355.12	-36.76	-391.88	0.094
	Zn-O6	2.236	-59.7008	-59.7008	56.7947	62.1597	-280.51	-22.97	-303.48	0.076
	N1-N2	2.676	-11.8153	-11.8153	9.6902	14.4061	292.25	-7.15	285.1	-0.025
ZnL_3	*CH···HC*	2.073	-0.2463	-0.2463	0.2553	0.2364	-0.52	-2.36	-2.88	0.821
	CH···N	2.746	-1.4669	-1.4669	*0.2553*	*0.2364*	-11.71	-2.26	-13.97	0.162
	C-C	1.496	-11.4046	-11.4046	0.5106	0.4729	96.79	-193.41	-96.62	2.002
	Zn-N2	2.229	-54.0400	-54.0400	49.8607	57.6798	-338.51	-32.93	-371.44	0.089
	Zn-N23	2.228	-54.0550	-54.0550	49.8744	57.6956	-338.79	-32.89	-371.68	0.088
	N2-N23	2.690	-11.7953	-11.7953	9.6755	14.3793	291.34	-7.24	284.11	-0.025

Table S8. IQA data for the CH•••HC interaction at MP2 level[a]

Form	$V_{cl}^{H,H}$ [b]	$V_{XC}^{H,H}$ [b]	$E_{int}^{H,H}$ [b]
ZnL	0.89	–3.25	–2.36
ZnL_2	0.85	–3.29	–2.44
ZnL_3	0.81	–3.46	–2.65

[a] Calculated as a MP2/6-311++G(d,p) single point calculation on DFT generated geometries at RX3LYP/ATZP level.
[b] All values in kcal·mol^{-1}

Some data computed for the free bpy ligand.

It is important and informative to consider now the kind and relative strength of some intramolecular interactions in s-*cis* and s-*trans* conformers of isolated bpy because in the former a CH--HC contact is observed. What follows, is a very brief description of the interactions most relevant to this work; a full account on fundamental properties controlling the preferential conformational state of the free bpy will be published soon. We found that two CH•••N interactions in the s-*trans* conformer contribute in stabilizing manner, for each $E_{\text{int}}^{\text{H,N}}$ = –14.84 kcal mol^{-1} ($V_{\text{cl}}^{\text{H,N}}$ = –10.57 kcal mol^{-1}). In the s-*cis* conformer $E_{\text{int}}^{\text{H,H}}$ = –3.03 kcal mol^{-1} ($V_{\text{cl}}^{\text{H,H}}$ = –0.05 kcal mol^{-1}) for CH•••HC and $E_{\text{int}}^{\text{N,N}}$ = +255.60 kcal mol^{-1} ($V_{\text{cl}}^{\text{N,N}}$ = +264.11 kcal mol^{-1}) for N--N were obtained at HF/6-311++G(d,p)/PCM. We also computed $E_{\text{int}}^{\text{H,H}}$ = –3.55 kcal/mol ($V_{\text{cl}}^{\text{H,H}}$ = –0.43 kcal mol^{-1}) for CH•••HC at the MP2 level. From these data one can conclude that (i) the nature of these interactions can be understood qualitatively already at HF and this correlates well with the same conclusion reported elsewhere,[1-3] (ii) the physical nature of the CH•••HC interaction in the s-*cis* conformer of bpy and metal complexes is very much the same (a dominant contribution comes from the exchange-correlation term), (iii) the CH•••HC interaction is the weakest, by far, among others in both conformers of bpy. Hence, just considering the strength of interactions, the preferential conformational state of bpy is controlled by (i) highly repulsive N--N contact (this is the interaction which makes the s-*cis* conformer energetically unstable) and (ii) two CH•••N interactions which re-enforce the stability of the s-*trans* conformer.

References

(1) Pendás, A. M.; Francisco, E.; Blanco, M. A.; Gatti, C. *Chem. Eur. J.* **2007**, *13*, 9362–9371.

(2) Francisco, E.; Pendás, A. M.; Blanco, M. A. *J. Chem. Theory Comput.* **2006**, *2*, 90–102.

(3) Pendás, A. M.; Blanco, M. A.; Francisco, E. *J. Comput. Chem.* **2007**, *28*, 161–184.

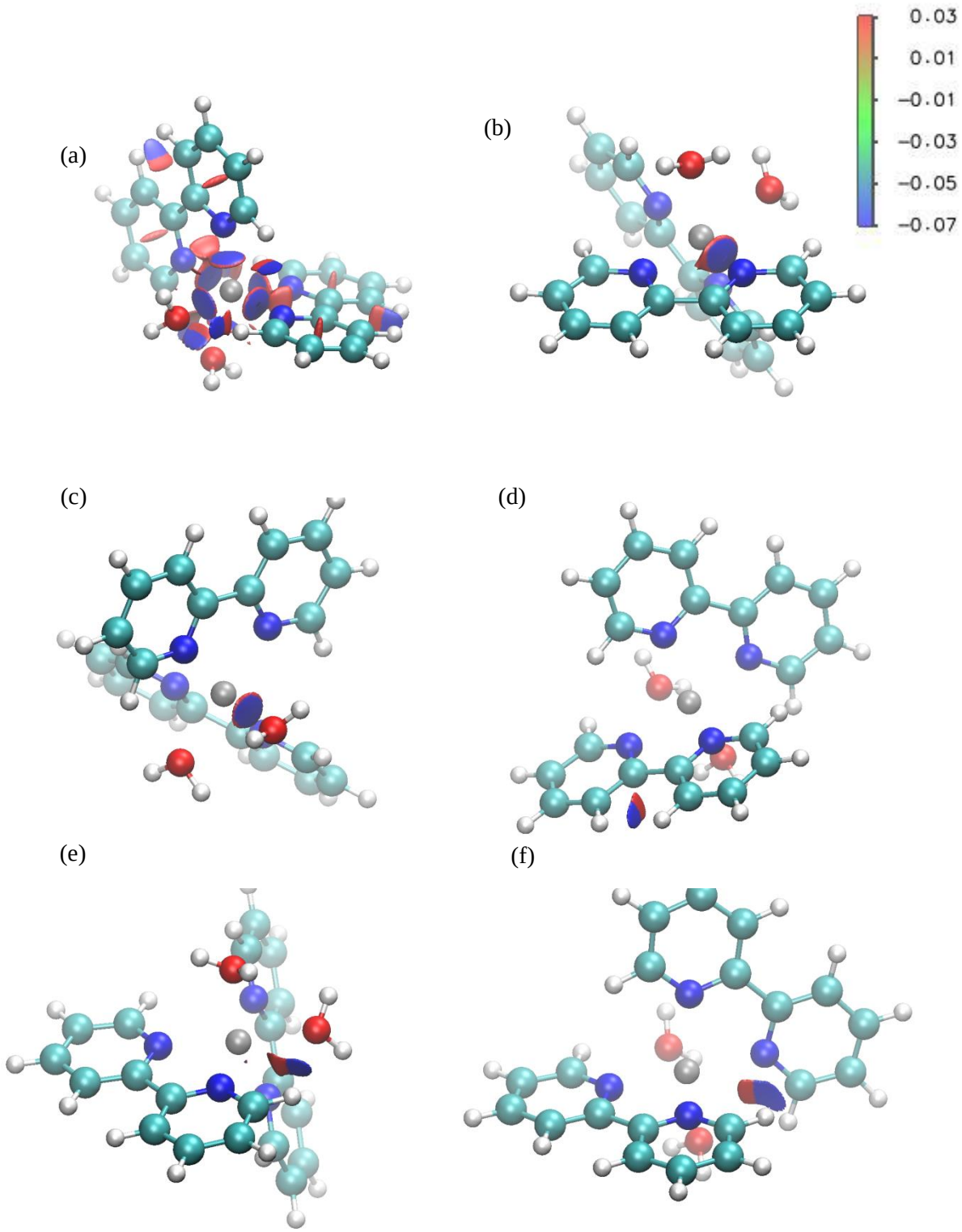

Figure S5. NCI Isosurfaces for all the interactions in ZnL_2. (a) All interactions. (b) Zn–N. (c) Zn–O. (d) CH•••HC. (e) CH•••O. (f) CH•••N. The surfaces indicate the reduced density gradient at an isovalue of 0.5 au. The colour scheme used, from blue, through green to red, reflects the following range –0.07 au < sign(λ_2) × ρ < 0.03 au.

(a)

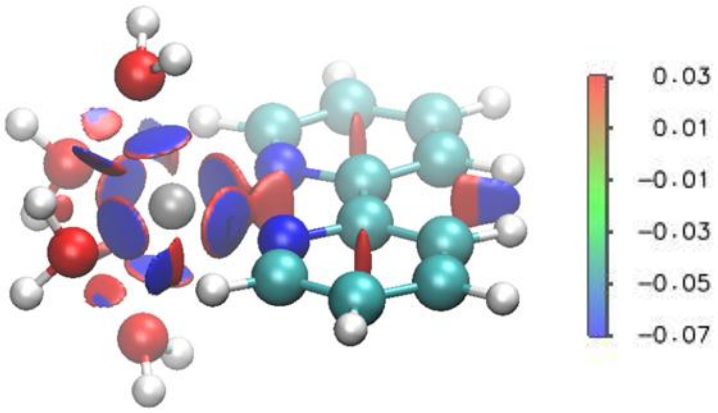

(b)

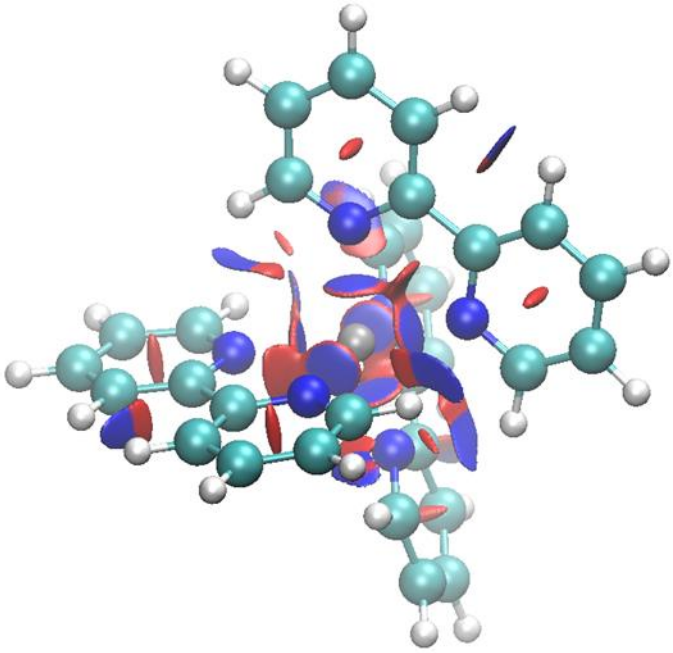

Figure S6. NCI isosurfaces for (a) ZnL and (b) ZnL_3. The surfaces indicate the reduced density gradient at an isovalue of 0.5 au. The colour scheme used, from blue, through green to red, reflects the following range –0.07 au < sign(λ_2) × ρ < 0.03 au.

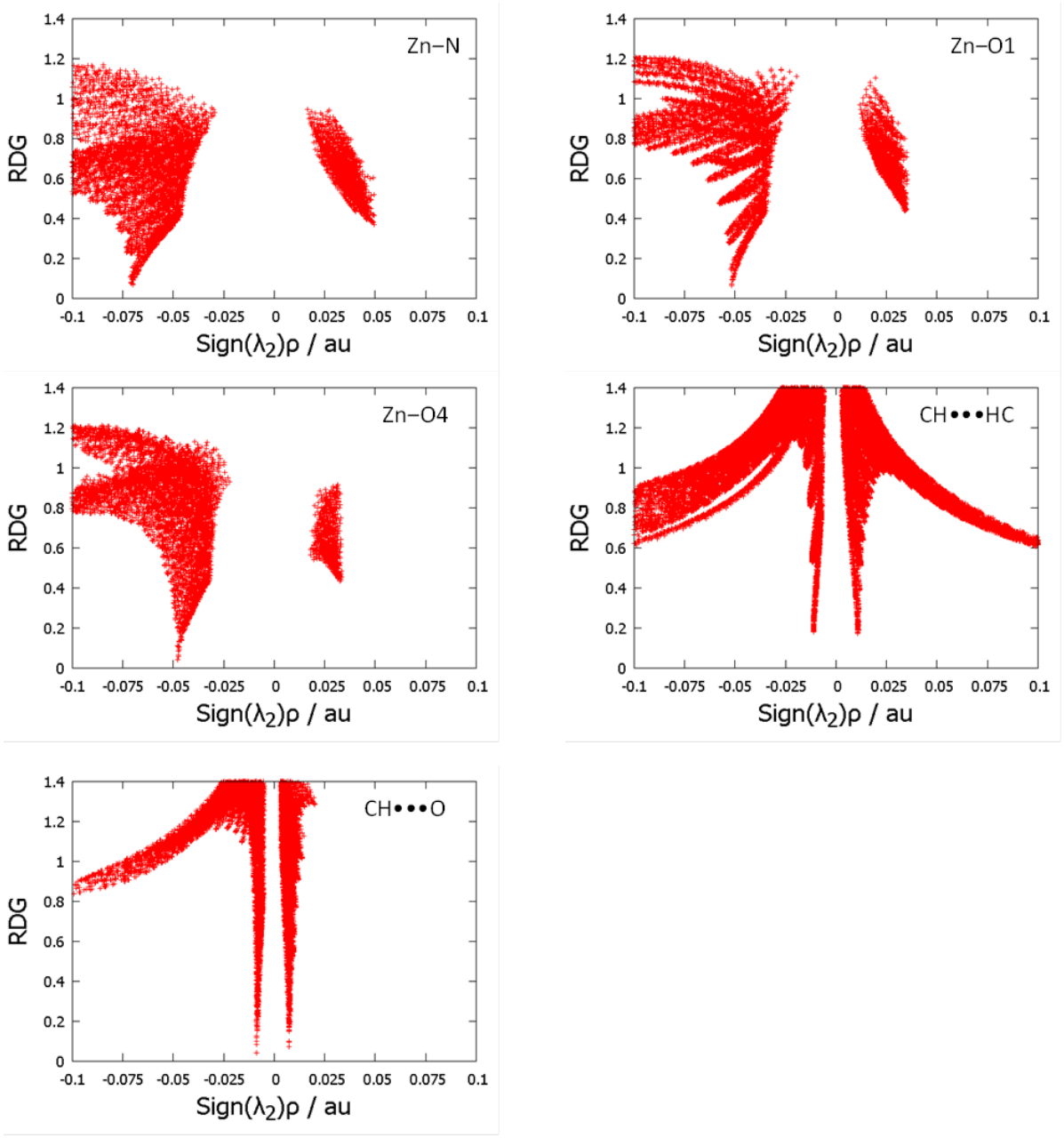

Figure S7. NCI-plots for interactions in ZnL.

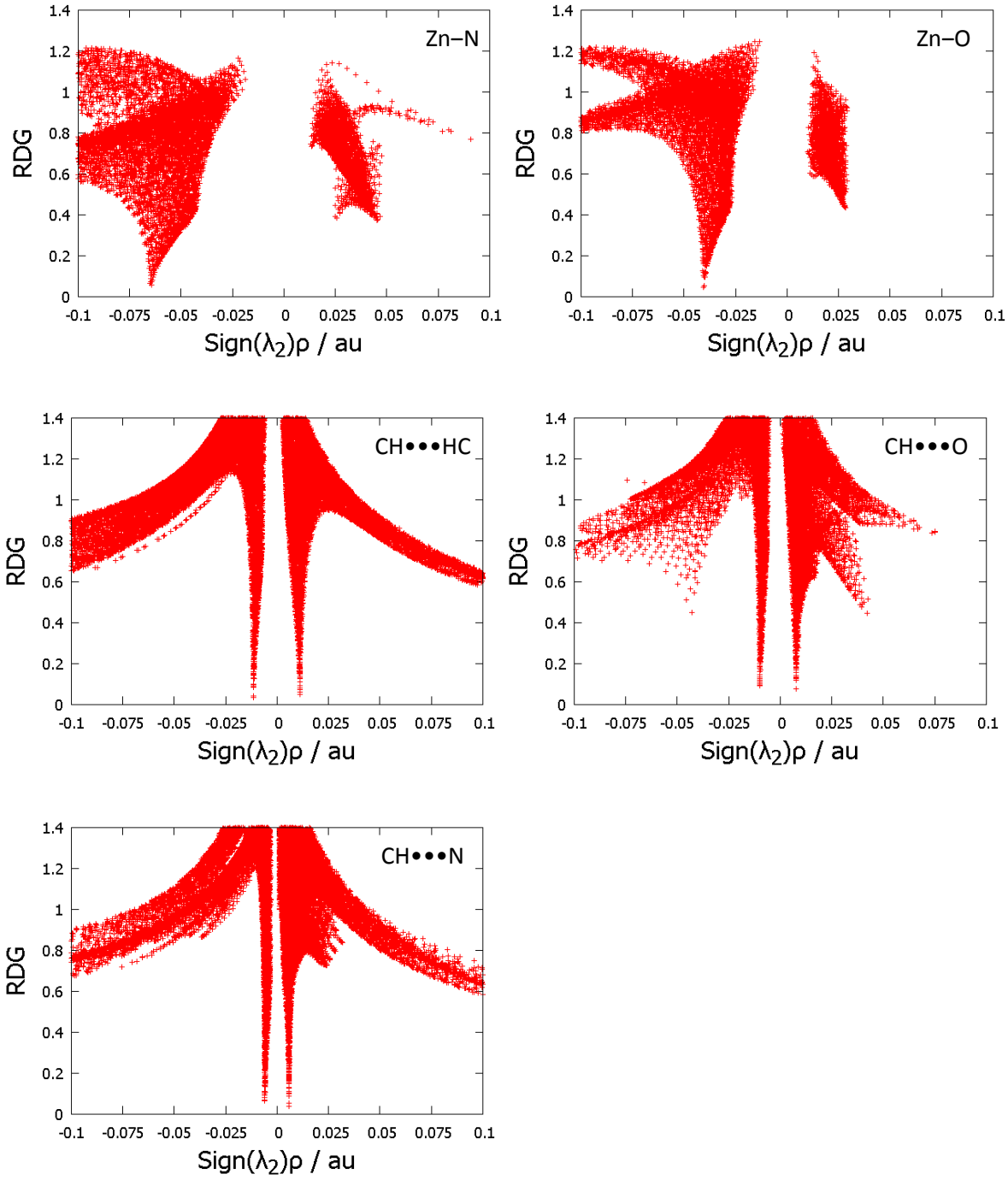

Figure S8. NCI-plots for all interactions in ZnL_2.

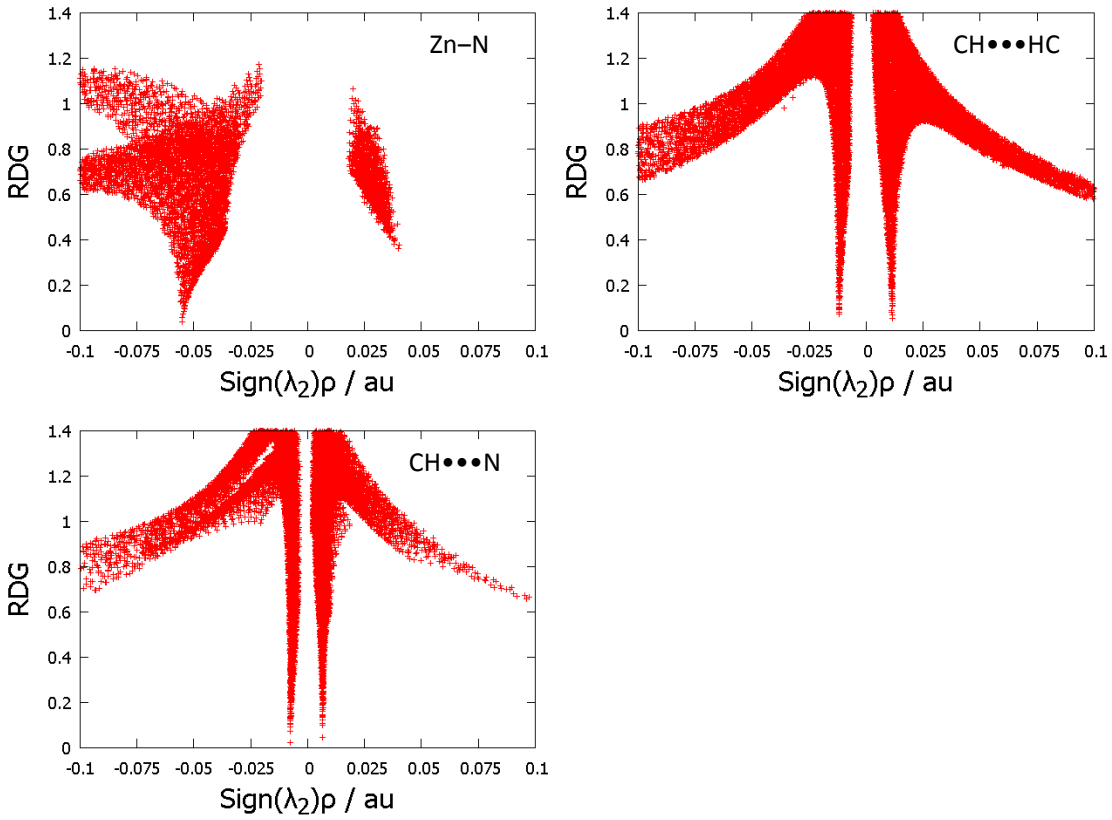

Figure S9. NCI-plots for interactions in ZnL_3.

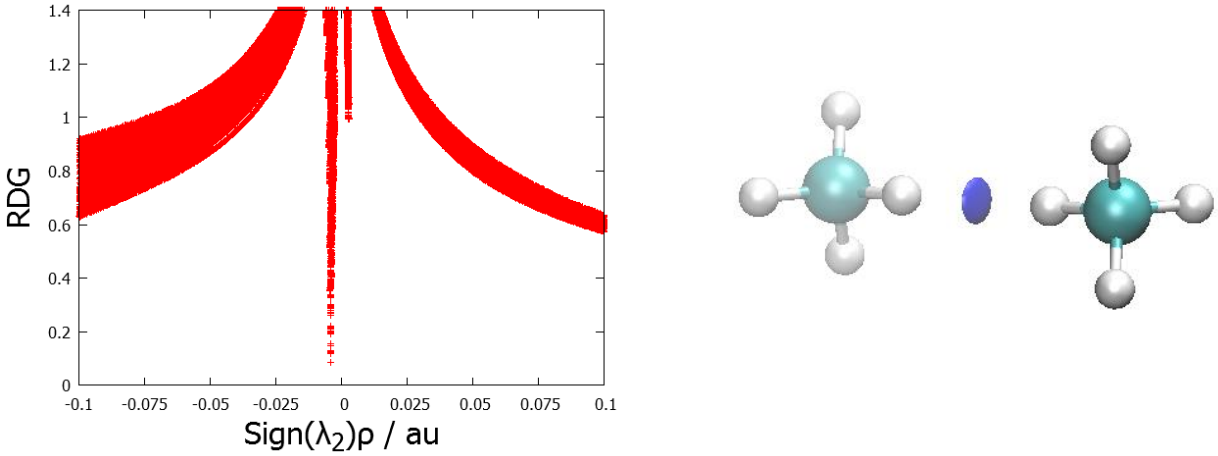

Figure S10. NCI-plot and associated isosurface (isovalue = 0.5 a.u.) for the head-on approach of a methane dimer. (–) $\rho_{ICP}^{H,H}$ = –0.0043 au, (+) $\rho_{ICP}^{H,H}$ = +0.0027 a.u. (at the B97-D level)

Table S9. NCI-plot data for ZnL, ZnL_2 and ZnL_3

Complex	Interaction	(–) ρ_{ICP}^{AB}	(+) ρ_{ICP}^{AB}
ZnL	Zn–N	-0.07030	
	Zn–O1	-0.05162	
	Zn–O4	-0.04786	
	CH•••HC	-0.01126	0.01084
	CH•••O	-0.00869	0.00736
	N•••N		0.02152
	Pyridine Rings		0.02395
ZnL_2	Zn–N	-0.06449	
	Zn–O	-0.04062	
	CH•••HC	-0.01155	0.01104
	CH•••O	-0.01007	0.00768
	CH•••N	-0.00596	0.00580
	N•••N		0.02082
	Pyridine Rings		0.02398
ZnL_3	Zn–N	-0.05520	
	CH•••HC	-0.01199	0.01134
	CH•••N	-0.00763	0.00663
	N•••N		0.01983
	Pyridine Rings		0.02406
	CH•••N Rings		0.00154

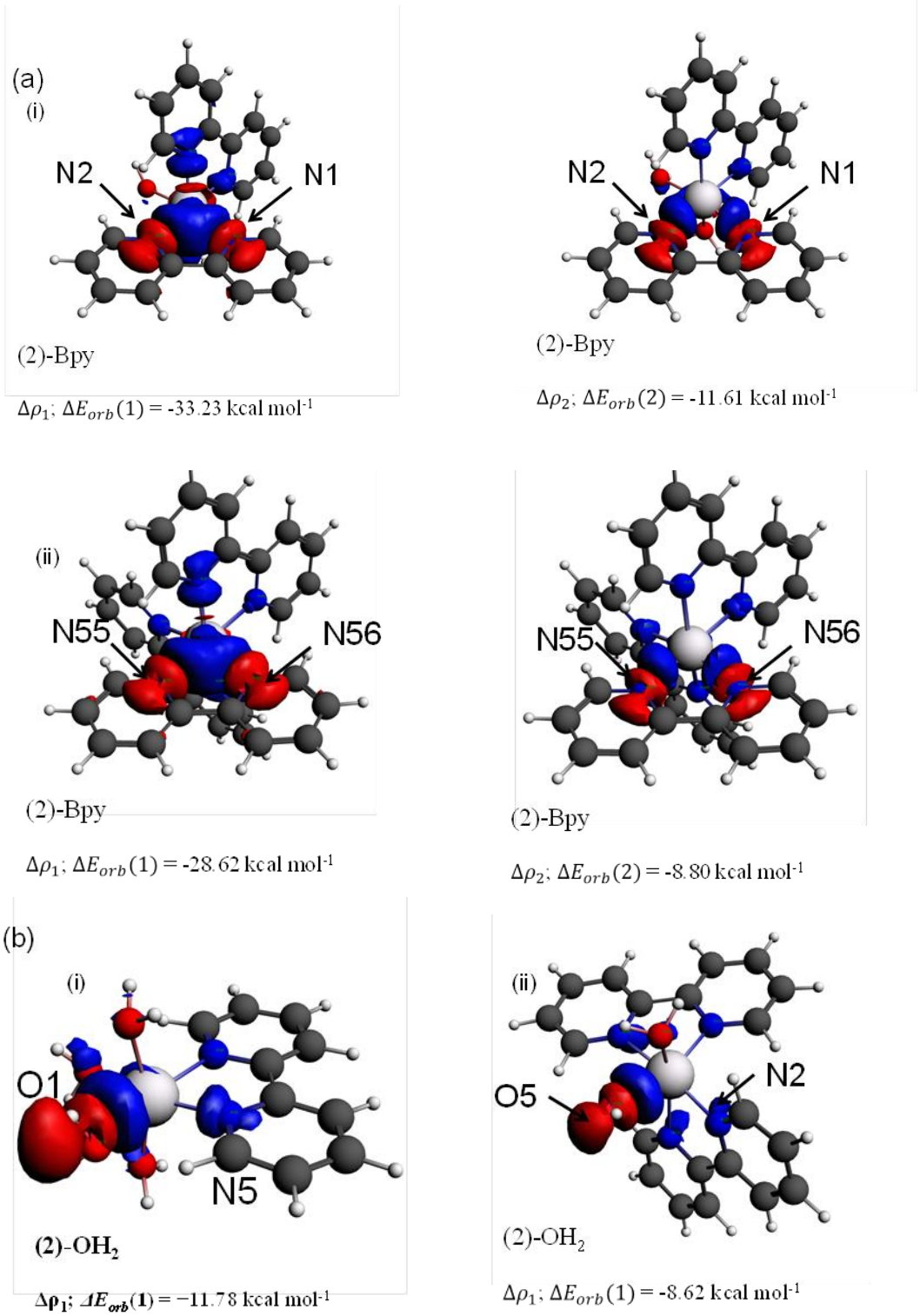

Figure S11. NOCV deformation densities for (a) Zn–N bonds in (i) ZnL_2 and (ii) ZnL_3, and (b) Zn–O bonds in (i) ZnL and (ii) ZnL_2.

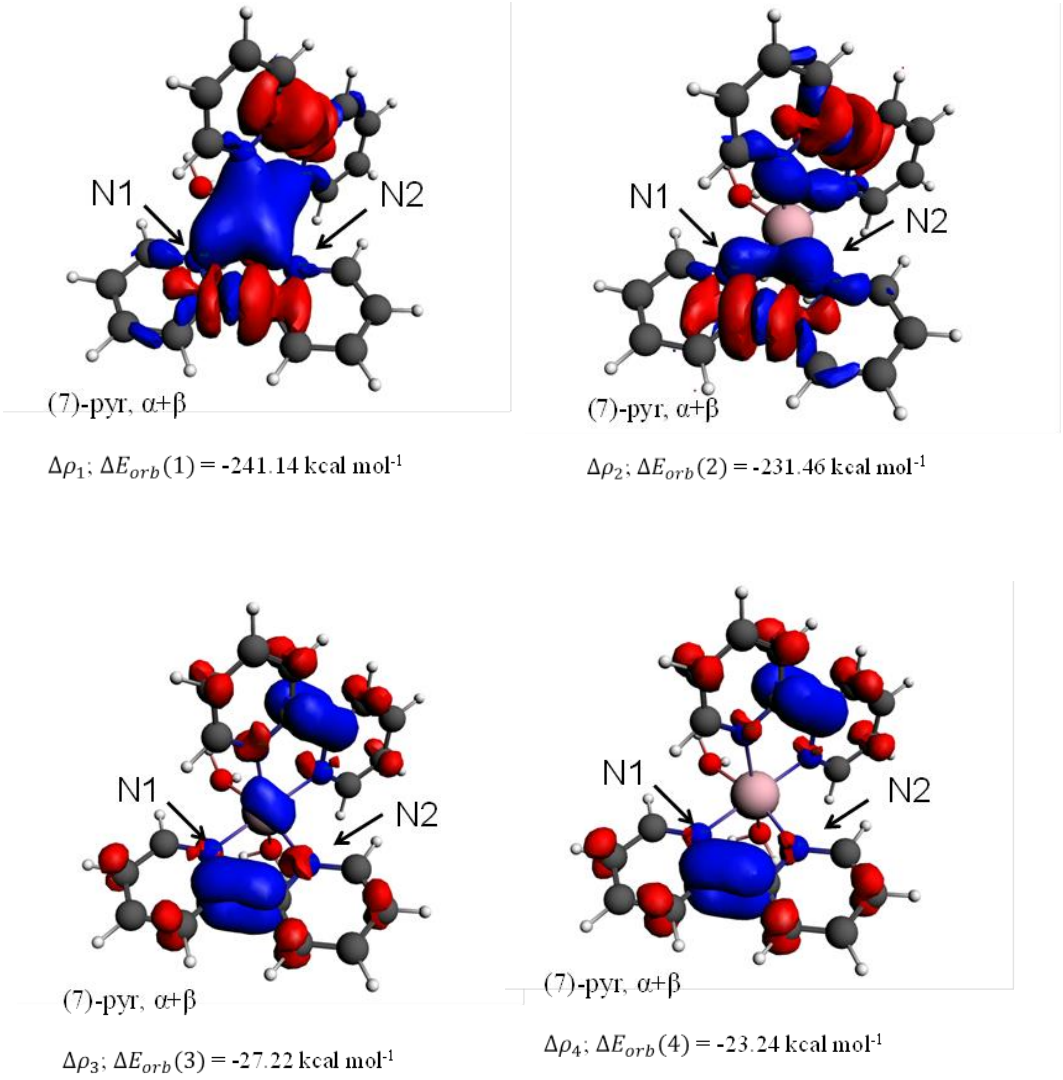

Figure S12. NOCV deformation densities for C–C bonds in ZnL_2 .

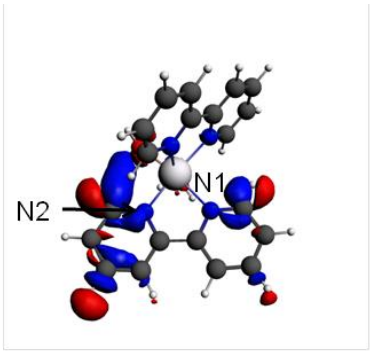

(2)-Bpy

$\Delta\rho_{18}$; $\Delta E_{orb}(18)$ = -0.28 kcal mol^{-1}

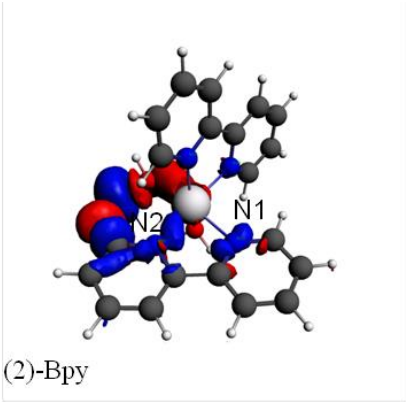

(2)-Bpy

$\Delta\rho_{15}$; $\Delta E_{orb}(15)$ = -1.11 kcal mol^{-1}

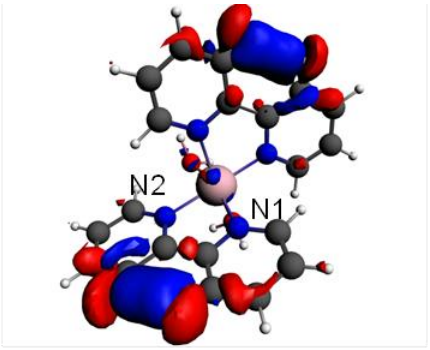

(7)-pyr, α+β

$\Delta\rho_{25}$; $\Delta E_{orb}(25)$ = -1.43 kcal mol^{-1}

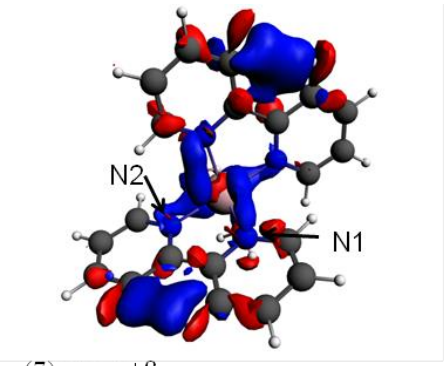

(7)-pyr, α+β

$\Delta\rho_{23}$; $\Delta E_{orb}(23)$ = -2.42 kcal mol^{-1}

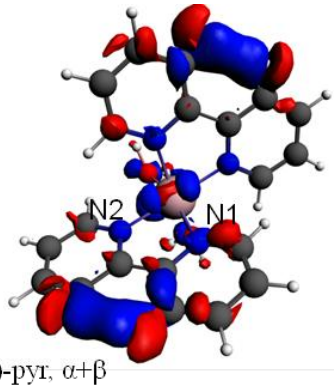

(7)-pyr, α+β

$\Delta\rho_{26}$; $\Delta E_{orb}(26)$ = -1.71 kcal mol^{-1}

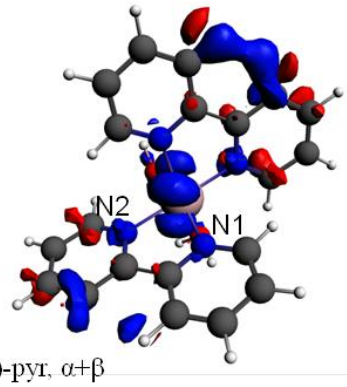

(7)-pyr, α+β

$\Delta\rho_{27}$; $\Delta E_{orb}(27)$ = -2.74 kcal mol^{-1}

Figure S13. NOCV deformation densities for CH•••O and CH•••HC interactions in ZnL_2.

Table S10. NOCV deformation densities describing all interactions in all ZnBPy complexes

Complex	Structural Bonds					Intramolecular interactions				
	Bond	**Fragmentation Scheme**	**$\Delta\rho_k$ channel**	**|NOCV Eigenvalue|** *(a.u.)*	**ΔE_{orb}^{k}** *(kcal·mol^{-1})*	**Interaction**	**Fragmentation scheme**	**$\Delta\rho_k$ channel**	**|NOCV Eigenvalue|** *(a.u.)*	**ΔE_{orb}^{k}** *(kcal·mol^{-1})*
ZnL	Zn–N	(2)-bpy	1	0.43715	-37.69	CH•••HC	(7)-pyr	21	0.06034	-2.45
			2	0.23906	-14.31			23	0.05304	-1.81
	Zn–O1	(2)-OH_2	1	0.26448	-11.78	CH•••O	(2)-bpy	12	0.06581	-1.82
	Zn–O2	(2)-OH_2	1	0.26261	-10.88			14	0.04664	-0.77
	Zn–O3	(2)-OH_2	1	0.26408	-11.78			16	0.04114	-0.38
	Zn–O4	(2)-OH_2	1	0.26296	-10.88					
	C–C	(7)-pyr	1	1.10324	-239.55					
			2	0.38952	-23.98					
ZnL_2	Zn–N1/N2	(2)-bpy	1	0.44706	-33.23	CH•••HC	(7)-pyr	23	0.05881	-2.42
			2	0.23805	-11.61			25	0.05533	-1.43
	Zn–N3/N4	(2)-bpy	1	0.44758	-33.37			26	0.05307	-1.71
			2	0.23803	-11.64			27	0.05101	-2.74
	Zn–O5	(2)-OH_2	1	0.23801	-8.62	CH•••O (N1/N2)	(2)-bpy	15	0.05571	-1.11
	Zn–O6	(2)-OH_2	1	0.237	-8.53			18	0.0419	-0.28
	C–C	(7)-pyr	1	1.10164	-241.14	CH•••O (N3/N4)	(2)-bpy	15	0.05595	-1.13
			2	1.0962	-231.46			18	0.04209	-0.26
			3	0.38961	-27.22					
			4	0.38654	-23.24	CH•••N (N1/N2)	(2)-bpy	17	0.04667	-0.58

Complex	Structural Bonds					Intramolecular interactions				
	Bond	**Fragmentation Scheme**	**$\Delta\rho_k$ channel**	**|NOCV Eigenvalue|** *(a.u.)*	**ΔE_{orb}^{k}** *(kcal·mol^{-1})*	**Interaction**	**Fragmentation scheme**	**$\Delta\rho_k$ channel**	**|NOCV Eigenvalue|** *(a.u.)*	**ΔE_{orb}^{k}** *(kcal·mol^{-1})*
						CH•••N (N3/N4)	(2)-bpy	17	0.04664	-0.58
ZnL_3	Zn–N55/N56	(2)-bpy	1	0.42853	-28.62	CH•••HC	(7)-pyr	26	0.05804	-2.04
			2	0.21834	-8.80			27	0.05793	-2.04
	Zn–N57/N58	(2)-bpy	1	-0.42898	-28.64			28	0.05604	-1.31
			2	-0.21828	-8.77			29	0.05427	-2.42
	Zn–N59/N60	(2)-bpy	1	0.42872	-28.62			30	0.05397	-2.60
			2	0.21819	-8.76					
	C–C	(7)-pyr	1	1.10	-241.54					
			2	1.09	-228.60					
			3	1.09	-228.57					
			4	0.38	-28.75					
			5	0.38	-22.79					
			6	0.38	-21.19					

[a] *k* refers to the numbering of NOCV channels, ordered according to the magnitude of each NOCV channel's eigenvalue.

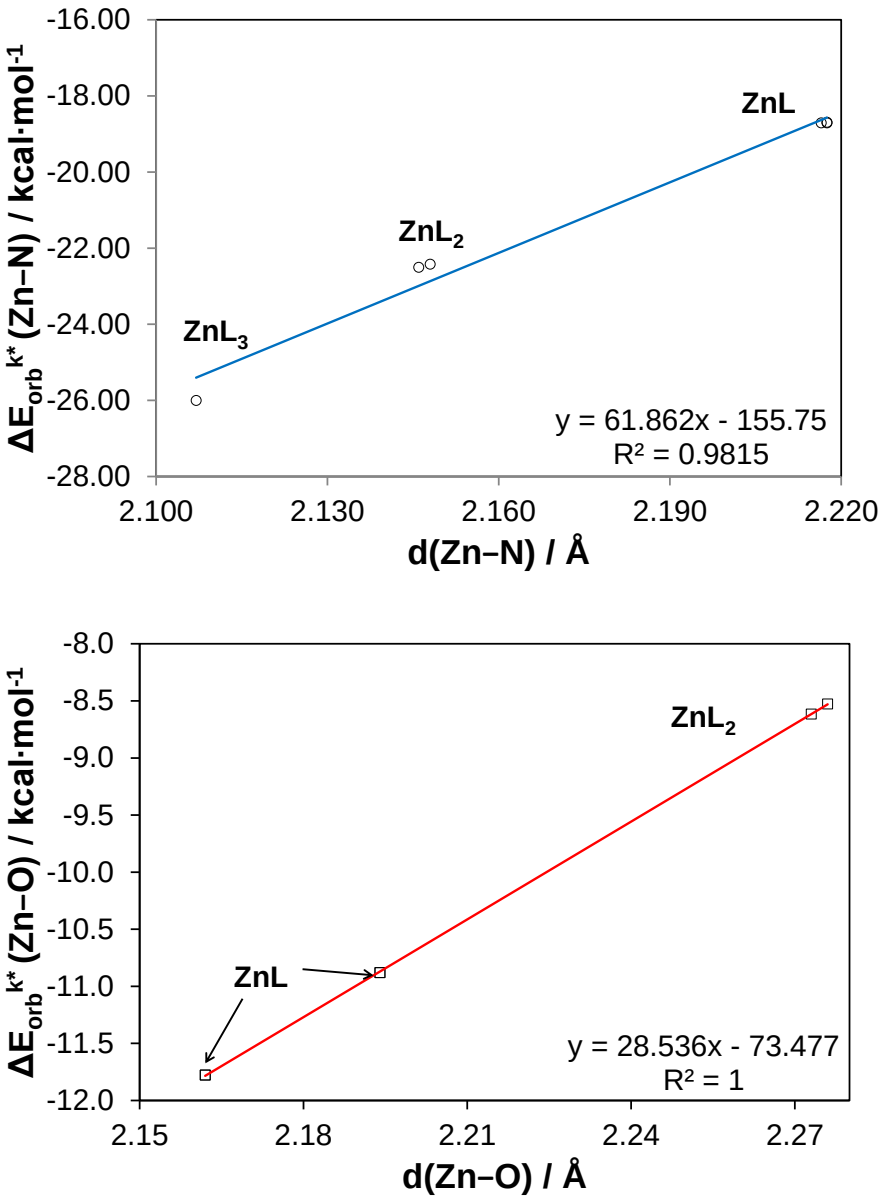

Figure S14. Relationship of the averaged orbital deformation energy per interaction with the interatomic distance for the indicated coordination bonds.

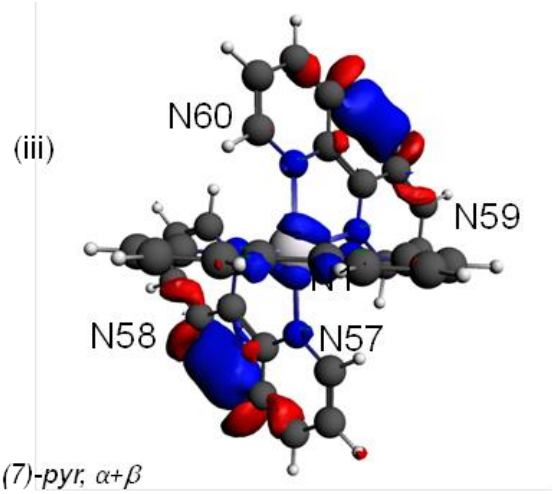

(7)-pyr, α+β
$\Psi^{26}_{-k,k}$; $\Delta E_{orb}{}^{k}$ = -2.04 kcal mol^{-1}
k = 0.05804 *au*, Isovalue = 0.0001 *au*
Exchange

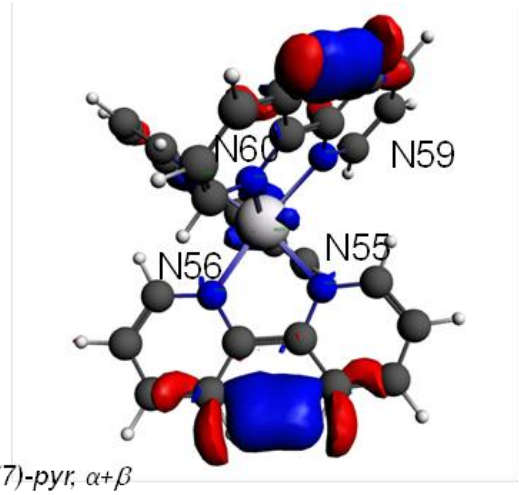

(7)-pyr, α+β
$\Psi^{27}_{-k,k}$; $\Delta E_{orb}{}^{k}$ = -2.04 kcal mol^{-1}
k = 0.05793 *au*, Isovalue = 0.0001 *au*
Exchange

Figure S15. Examples of NOCV deformation densities for CH•••HC interactions in ZnL_3.

Table S11. Calculating ΔE_{orb}^{k*} for CH•••HC interactions

	$\Delta\rho_k$ **channel**	ΔE_{orb}^{k} *(kcal mol^{-1})*	m[a]	$(\Delta E_{orb}^{k}/m)$
ZnL	21	-2.45	1	-2.45
	23	-1.81	1	-1.81
	sum	*-4.27*	ΔE_{orb}^{k*}	***-4.27***
ZnL_2	23	-2.42	2	-1.21
	25	-1.43	2	-0.72
	26	-1.71	2	-0.86
	27	-2.74	1	-2.74
	sum	*-8.30*	ΔE_{orb}^{k*}	***-5.52***
ZnL_3	26A	-1.02	*2*	-0.51
	27A	-1.02	*2*	-0.51
	28A	-0.65	*3*	-0.22
	29A	-1.22	*1*	-1.22
	30A	-1.29	*2*	-0.65
	26B	-1.02	*1*	-1.02
	27B	-1.02	*2*	-0.51
	28B	-0.65	*3*	-0.22
	29B	-1.20	*1*	-1.20
	30B	-1.30	*1*	-1.30
	sum	*-10.41*	ΔE_{orb}^{k*}	***-7.36***

[a] *m* refers to the number of interactions showing density deformations for a specific NOCV channel

ΔE_{Orb}^{k*} was calculated by visually inspecting each NOCV channel in order to approximate the number of described interactions and then normalizing ΔE_{orb}^{k} by dividing by the number of interactions. The sum of each such normalized ΔE_{orb}^{k} gives ΔE_{orb}^{k*} for each interaction.

Table S12. Calculating ΔE_{orb}^{k*} for CH•••O interactions

	$\Delta\rho_k$ channel	ΔE_{orb}^{k} (kcal mol^{-1})	m[a]	$(\Delta E_{orb}^{k}/m)$
ZnL	12	-1.82	2	-0.91
	14	-0.77	2	-0.38
	16	-0.38	2	-0.19
	sum	*-2.96*		*-1.48*
ZnL_2	15	-1.11	1	-1.11
N1-N2	17	-0.58	2	-0.29
	18	-0.28	1	-0.28
	sum	*-1.97*		*-1.68*
ZnL_2	15	-1.13	1	-1.13
N3-N4	17	-0.58	2	-0.29
	18	-0.26	1	-0.26
	sum	*-1.97*		*-1.68*

[a] *m* refers to the number of interactions showing density deformations for a specific NOCV channel

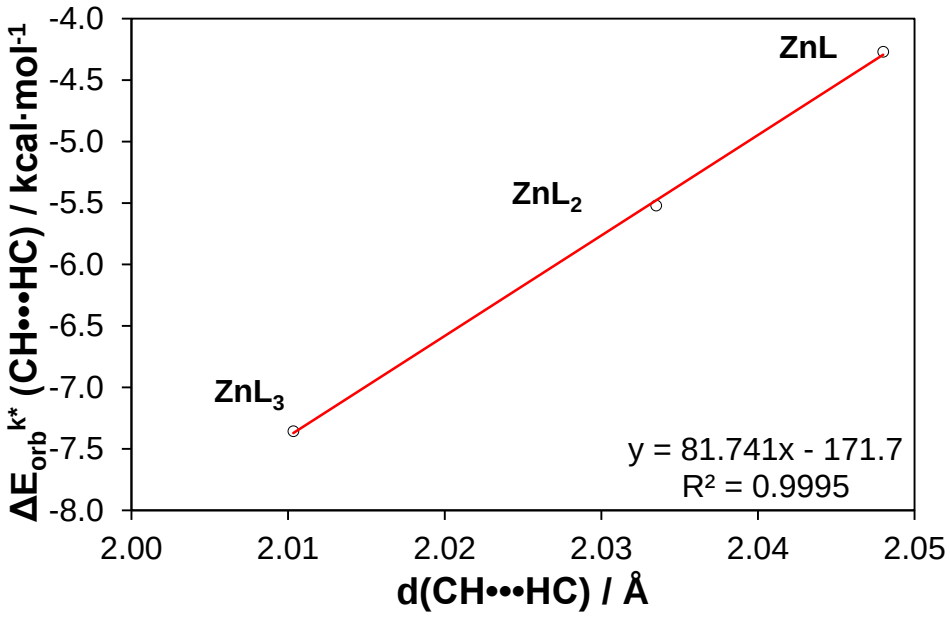

Figure S16. Relationship of the averaged orbital deformation energy per interaction with the interatomic distance for the CH•••HC interaction.

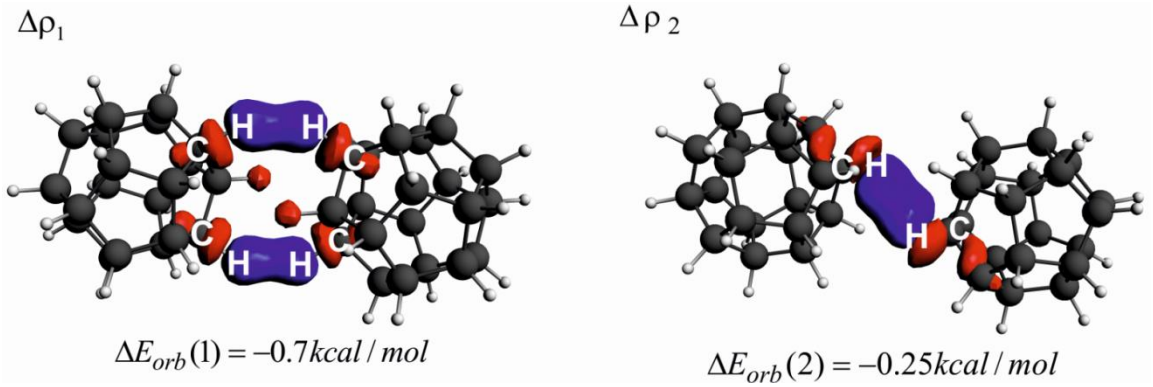

Figure S17. Dominating NOCV deformation densities, $\Delta\rho_1$, $\Delta\rho_2$ with the corresponding energies, $\Delta E_{orb}(1)$, $\Delta E_{orb}(2)$, describing CH--HC contacts in dimer of dodecahedrane.

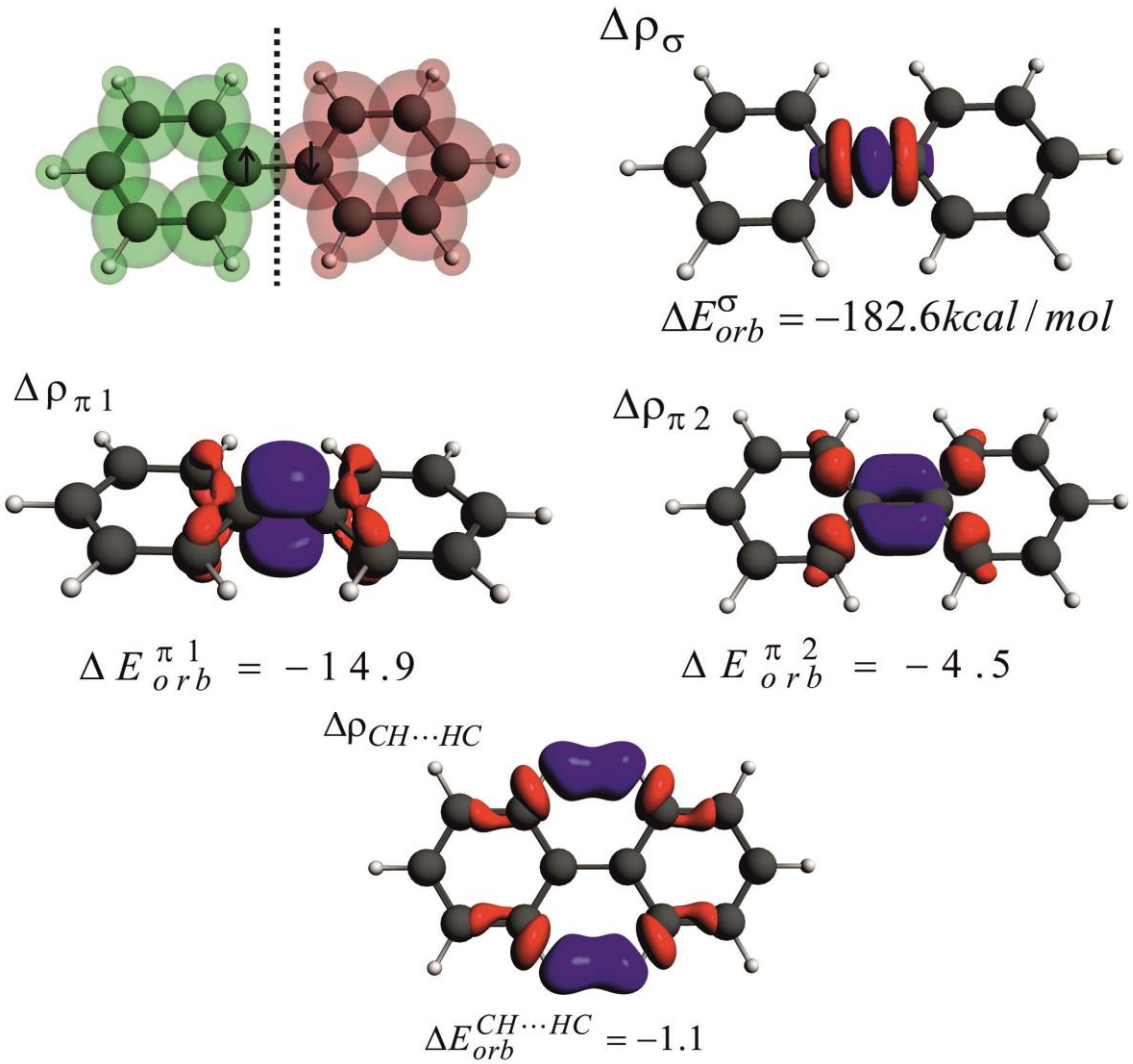

Figure S18. Leading deformation density channels describing the interactions between two phenyl rings (carrying opposite spin polarization) in planar biphenyl.

Table S13. ETS-NOCV description of deformation energies in four-fragment resolution

	ΔE_{total} [a]	ΔE_{elstat} [a]	ΔE_{orb} [a][b]	$\Delta E_{orb}(\pi)$ [b]	$\Delta E_{dispersion}$ [a]	ΔE_{Pauli} [a]	ΔE_{orb}(rest) [b]	$\Delta E_{orb}(\sigma)$ [b]
ZnL	-392.86	-345.16	-182.03	-18.24	-20.00	154.33	-35.75	-128.04
ZnL_2	-432.01	-367.87	-203.74	-39.60	-24.57	164.17	-38.14	-126.20
ZnL_3	-464.37	-386.02	-215.58	-49.10	-31.57	168.80	-45.58	-120.90

[a] $\Delta E_{total}=\Delta E_{elstat}+\Delta E_{pauli}+\Delta E_{orb}+\Delta E_{dispersion}$ (BLYP-D3/TZP),
[b] $\Delta E_{orb} = \Delta E_{orb}(\sigma)+ \Delta E_{orb}(\pi)+ \Delta E_{orb}$(rest)
All values in kcal mol^{-1}.

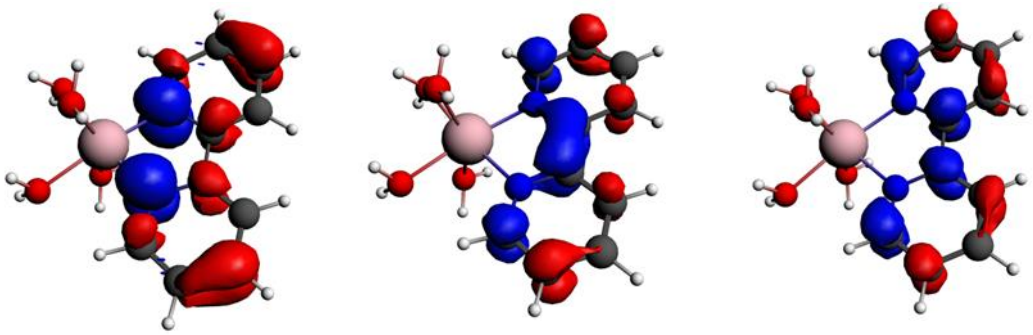

ΔE_{orb} (π1) = -10.3 kcal mol^{-1} ΔE_{orb} (π2) = -4.4 kcal mol^{-1} ΔE_{orb} (π3) = -3.54 kcal mol^{-1}

Figure S19. NOCV π-contributions for ZnL. ΔEorb(π)= ΔEorb(π1)+ ΔEorb(π2)+ ΔEorb(π3). Isosurface = 0.0005 au.

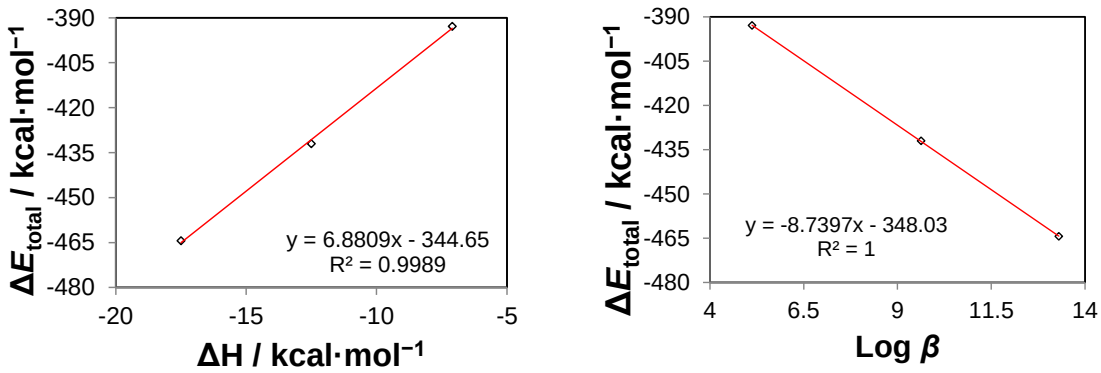

Figure S20. Relationships between ETS-defined total interaction energy and indicated experimental data for the formation of ZnL_n complexes.

Table S14. Calculated ^{1}J(C–H) coupling constants

	^{1}J(C–H) (CH•••HC) BP86/TZ2P	^{1}J(C–H) (CH•••HC) X3LYP/TZ2P	^{1}J(C–H) (CH•••O) BP86/TZ2P	^{1}J(C–H) (CH•••N) BP86/TZ2P
ZnL	159.97 (Hz)	177.06 (Hz)	174.72	---------
ZnL_2	158.44 (Hz)	175.72 (Hz)	174.46	170.59
ZnL_3	156.68 (Hz)	173.87 (Hz)	--------	165.75

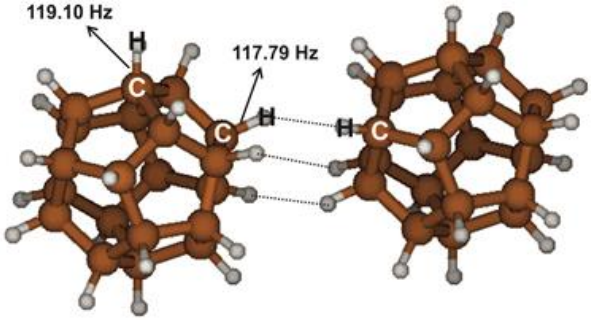

Figure S21. ^{1}J(C–H) coupling constants for the CH•••HC interaction in dodecahedron.

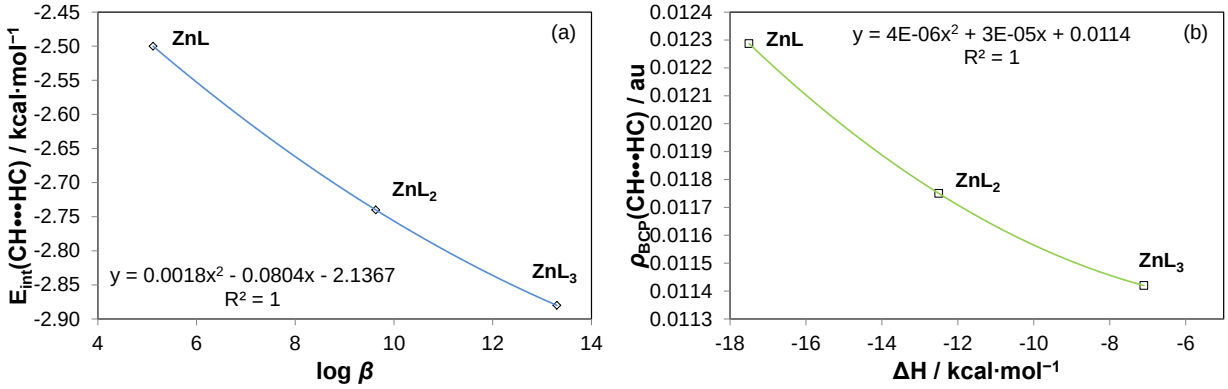

Figure S22. Relationship between IQA-defined interaction energy, $E_{int}^{H,H}$, and log β_n - part (a), whereas ρ_{BCP} vs. ΔH_f is shown in part (b); both for the CH•••HC interactions in ZnL_n.

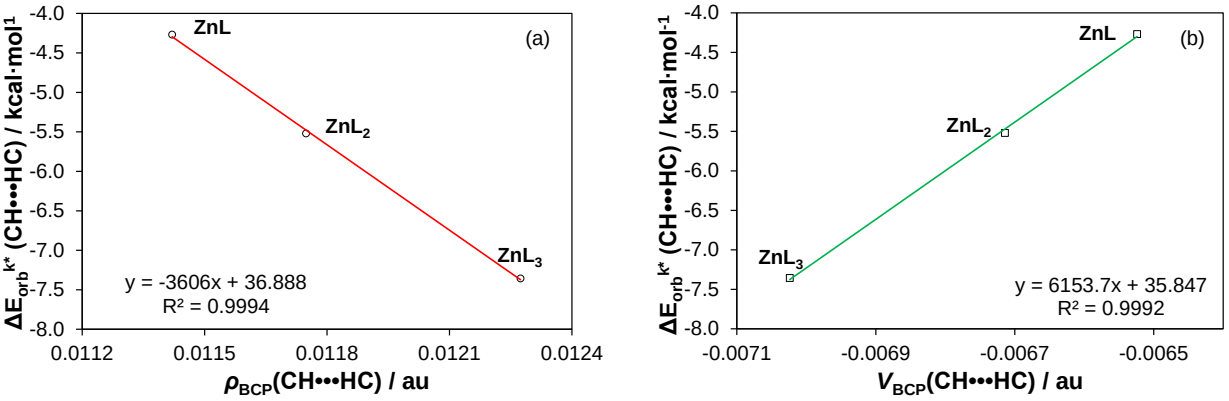

Figure S23. Relationship between NOCV orbital interaction energy and topological properties a) ρ_{BCP} and b) V_{BCP} for the CH•••HC interactions in ZnL_n.